2017

UTILIZATION OF EMPIRICAL MODELS TO DETERMINE THE BULK PROPERTIES OF COMPRESSED SOUND ABSORPTIVE MATERIALS

Ruimeng Wu
University of Kentucky, ruimengwu@uky.edu
Digital Object Identifier: https://doi.org/10.13023/ETD.2017.488

STUDENT AGREEMENT:

I represent that my thesis or dissertation and abstract are my original work. Proper attribution has been given to all outside sources. I understand that I am solely responsible for obtaining any needed copyright permissions. I have obtained needed written permission statement(s) from the owner(s) of each third-party copyrighted matter to be included in my work, allowing electronic distribution (if such use is not permitted by the fair use doctrine) which will be submitted to UKnowledge as Additional File.

I hereby grant to The University of Kentucky and its agents the irrevocable, non-exclusive, and royalty-free license to archive and make accessible my work in whole or in part in all forms of media, now or hereafter known. I agree that the document mentioned above may be made available immediately for worldwide access unless an embargo applies.

I retain all other ownership rights to the copyright of my work. I also retain the right to use in future works (such as articles or books) all or part of my work. I understand that I am free to register the copyright to my work.

REVIEW, APPROVAL AND ACCEPTANCE

The document mentioned above has been reviewed and accepted by the student's advisor, on behalf of the advisory committee, and by the Director of Graduate Studies (DGS), on behalf of the program; we verify that this is the final, approved version of the student's thesis including all changes required by the advisory committee. The undersigned agree to abide by the statements above.

Ruimeng Wu, Student

Dr. David W. Herrin, Major Professor

Dr. Haluk E. Karaca, Director of Graduate Studies

UTILIZATION OF EMPIRICAL MODELS TO DETERMINE THE BULK PROPERTIES OF COMPRESSED SOUND ABSORPTIVE MATERIALS

THESIS

A thesis submitted in partial fulfillment of the
requirements for the degree of Master of Science
in Mechanical Engineering in the College of Engineering
at the University of Kentucky

By

Ruimeng Wu

Lexington, Kentucky

Director: Dr. David W. Herrin, Professor of Mechanical Engineering

Lexington, Kentucky

2017

ABSTRACT OF THESIS

UTILIZATION OF EMPIRICAL MODELS TO DETERMINE THE BULK PROPERTIES OF COMPRESSED SOUND ABSORPTIVE MATERIALS

Empirical models based on flow resistivity are commonly used to determine the bulk properties of porous sound absorbing materials. The bulk properties include the complex wavenumber and complex characteristic impedance which can be used directly in simulation models. Moreover, the bulk properties can also be utilized to determine the normal incidence sound absorption and specific acoustic impedance for sound absorbing materials of any thickness and for design of layered materials. The sound absorption coefficient of sound absorbing materials is measured in an impedance tube using wave decomposition and the measured data is used to determine the flow resistivity of the materials by least squares curve fitting to empirical equations. Results for several commonly used foams and fibers are tabulated to form a rudimentary materials database. The same approach is then used to determine the flow resistivity of compressed sound absorbing materials. The flow resistivities of the compressed materials are determined as a function of the compression ratio. Results are then used in conjunction with transfer matrix theory to predict the sound absorptive performance of layered compressed absorbers with good agreement to measurement.

KEYWORDS: Passive Noise Control, Acoustic Impedance, Flow Resistivity, Sound Absorbing Materials, Rudimentary Database, Compressed Materials.

Ruimeng Wu
Student's Signature

5th November, 2017

.

UTILIZATION OF EMPIRICAL MODELS TO DETERMINE THE BULK PROPERTIES OF COMPRESSED SOUND ABSORPTIVE MATERIALS

By

Ruimeng Wu

Dr. David W. Herrin
Director of Thesis

Dr. Haluk E. Karaca
Director of Graduate Studies

5th November, 2017

.

ACKNOWLEDGEMENTS

Foremost, I would like to express my deepest gratitude to my advisor Professor David Herrin, for his excellent guidance, motivation, patience, providing me with an excellent atmosphere for doing research, and offering me opportunities to get practical training in the industry. I would like to thank my co-advisor Professor Tingwen Wu for his encouragement and advice on my research work. Special thanks goes to Professor John Baker, who was willing to participate in my final defense committee and provide valuable comments and suggestions.

I would like to thank James Haylett for offering me the summer internship opportunities at Commercial Vehicle Group in 2015. I would also like to thank Charles Moritz for offering me the summer internship opportunities at Blachford in 2016. Both internships gave me a lot of working experience and taught me different kind of skills.

I would like to thank my fellows and friends in the Vibro-Acoustics Group: Wanlu Li, Gong Cheng, Yitian Zhang, Peng Wang, Weiyun Liu, Keyu Chen, Shujian He, Jundong Li, Caoyang Li, Nan Zhang, Jonathan Chen, Shishuo Sun and Xin Hua for all the fun we have had in the past several years and the selfless help in my research.

I would like to thank my lovely roommates, Ruiqian Zhan, Xie jin, Jiaji Liang and Yixuan Zou for taking care of me and the great time we had together.

I would also like to thank my parents, two younger sisters. They were always supporting me and encouraging me with their best wishes.

Finally, I would like to thank my wife, Mengdi Liu. She was always there cheering me up and stood by me through the good times and bad.

TABLE OF CONTENTS

.

LIST OF FIGURES

.

LIST OF TABLES

Chapter 1 Introduction

1.1 Background

Sound absorbing materials are the most commonly used approach to reduce noise in vehicles and buildings. Applications include but are not limited to small pumps for healthcare equipment, engine and passenger compartments in heavy equipment, and auditoria in buildings. For the most part, porous absorbers are used because they offer good performance and are inexpensive.

Though there are numerous porous absorbers available commercially, there are two primary categories: fibers and foams. Examples of sound absorptive fibers include glass fiber, rockwool, and polyester fiber. Compressed fiber is used a great deal in ventilation ducts for heating and air conditioning because it offers adequate heat insulation and is not combustible. It is also commonly used in under hood applications for the aforementioned reasons and because it is durable.

Figure 1.1 A wide variety of sound absorbing materials.

The most widely used sound absorptive foams are polyesters, polyether, and melamine. Polyester and polyether foams are highly flammable and so applications are limited. Melamine is acceptable at elevated temperatures but degrades in humid environments. For these reasons, a cover is commonly placed over a foam to protect it.

In addition to these traditional absorptive materials, newer materials like micro-perforated panels and sound absorptive fabrics are being employed in a number of applications. Though these sound absorptive materials have their place, they are considerably more expensive than fibers and foams and are used in niche applications.

Sound absorption occurs when sound energy is converted to heat through either mechanical damping or viscous dissipation as a sound wave propagates through a medium. Mechanical damping is important at low frequencies. It is difficult to model this effect and the resulting sound absorption is low. Viscous dissipation is the more important mechanism in the middle and high audible frequency ranges. Dissipation occurs as a result of friction between the oscillating or pulsating air and the solid matrix. Hence, sound absorption is more effective at higher frequencies where the acoustic particle velocity is higher.

Zwikker and Koston (1949) began the work on developing a phenomenological approach to characterize sound absorbing materials in the 1940's. A decade later, Biot (1956) developed a theory for the propagation of elastic waves in porous media that is still largely used today. Several decades later, Johnson et al. (1987),

.

Champoux (1991) and Allard (1993) (abbreviated as JCA) used measurable material properties like porosity, static flow resistivity, tortuosity, viscous characteristic length and thermal characteristic length to describe the viscous and thermal effect of the elastic porous material absorption at the macroscopic scale. The five Biot parameters can be measured directly based on their physical definitions. However, measurement requires dedicated equipment for each parameter (Pan and Jackson 2009).

The primary disadvantage of JCA is that the aforementioned properties are difficult to measure with the exception of the flow resistivity. Flow resistivity is simply $\Delta p/ut$ where Δp is the static pressure drop, u is the flow rate, and t is the thickness of the sound absorber. Mechel (1988) discovered that the sound absorption for various bulk densities of rock wool when plotted versus the parameter $\rho f/\sigma$ (where ρ is the density of air and f is the frequency) all generally lie on the same curve. This eventually led to the development of empirical formulas to characterize the complex wavenumber and characteristic impedance that were based on the flow resistivity alone. Empirical formulas have been developed by Delaney and Bazley (1970), Dunn and Davern (1986), Wu (1988), Mechel (1988), Miki (1990) and Garai and Pompoli (2005). These empirical equations take on the same algebraic form but their constants differ.

The empirical relationships between the acoustical properties and flow resistivity are easily utilized because the measurement of flow resistivity is straightforward. The measurement for flow resistivity is detailed in the ASTM C522 standard (2009). One possible limitation is that only a small subset of the sound absorbing materials

commercially available have been used to develop the empirical equations. Some question remains whether the equations are transferable to similar materials from different manufacturers than those used to originally develop the empirical equations. Bearing this in mind, several researchers (Braccecesi and Bracciali, 1997, Simón, et al. 2006, Atalla and Panneton, 2005) have recommended measuring the sound absorption or reflection coefficient in an impedance tube and then applying a least squares curve fit to minimize the errors between the measured properties and those calculated using either the phenomenological or empirical equations (inverse characterization). Sound absorption or reflection coefficient is measured in an impedance tube according to ASTM E1050 (2012).

A considerable body of work has been conducted related to inverse characterization using the phenomenological equations (JCA model). Panneton and Olny (2006) assume the dynamic density, open porosity and static flow resistivity of the sample are known or measured, and then an analytical solution is developed from the Johnson et al. (1987) model to determine geometrical tortuosity and viscous characteristic length. Zieliński (2015) used an inverse method to characterize sound absorbing rigid frame porous media based on direct measurement of the surface impedance of the rigid frame porous sample. Atalla and Panneton (2005) identified the parameters of the JCA model using an impedance tube to measure the surface impedance of the porous sample. Since the open porosity and flow resistivity can be determined with acceptable accuracy using standard techniques, only the tortuosity and viscous and thermal characteristic length need to be known. A cost function for the surface impedance

.

based on the three unknown properties is developed and the three unknown properties are calculated via optimization. Although the phenomenological model can describe the porous material more accurately, curve fitting to the phenomenological model is far more complex than the empirical model. In the JCA model, there are five unknown parameters that need to be identified. Three of the parameters (porosity, static flow resistivity, and bulk modulus for the solid) are commonly measured directly since they are easier to obtain in the lab. Following this the other two parameters can be curve fitted (Panneton and Olny, 2006). Using the ESI VA-One software, the measured sound reflection coefficient can be input and the 5 parameters are curve fitted. Curve fitting is conducted in three different frequency ranges (low, medium, and high) to determine the 5 unknown parameters (Atalla and Panneton, 2005). Though practicable, it is much easier to curve fit using the empirical relationships based on flow resistivity since only one variable needs to be determined.

1.2 Objectives

There are two primary objectives to the research documented in this thesis. The first is to develop a rudimentary materials database based on curve fitted flow resistivity which can be used as a tool by noise control engineers in the absence of other information. Flow resistivity and impedance tube measurements and associated curve fits are used to develop a database of flow resistivities for a subset of the materials commonly used in industry. Setting up a rudimentary materials database can increase the efficiency of noise control engineers since the acoustic performance of the materials can be determined from the respective flow

.

resistivities without additional laboratory measurements. Engineers can layer materials and customize the sound absorber for a particular application. Results for several commonly used foams and fibers are tabulated in the form a rudimentary materials database that can be expanded on in the future.

The second and more impactful objective is to study the effect of compression on sound absorbing materials. The flow resistivity of compressed samples is procured using the aforementioned curve fitting approach. Once the flow resistivity is known, an equation relating the flow resistivity to the compression ratio of the material is established experimentally. The noise control engineer can use this relationship to determine suitable properties for a compressed sound absorbing material. These properties can be used to predict the sound absorptive performance a priori and be utilized or used in numerical simulation models.

1.3 Organization

This thesis is organized in the following manner. Chapter 1 introduces the need for this research and establishes the two primary objectives: development of 1) a rudimentary materials database and 2) expressions relating the flow resistivity to the compression ratio for some common sound absorbing materials.

Chapter 2 surveys the different impedance tube methods for measuring the sound absorptive properties. In addition, the standard method for determining the flow resistivity is described. The empirical equations relating the bulk properties to the flow resistivity are also surveyed. Determination of the sound absorption from the bulk properties is also described.

.

In Chapter 3, an introductory materials database is developed based on flow resistivity. Flow resistivity is obtained by measuring the sound absorption in an impedance tube and then least square curve fitting to an appropriate empirical equation. Different processing schemes for performing the curve fit are discussed and compared. Results are tabulated for a range of fibers and plastic foams. The flow resistivity from the database is used to predict layered sound absorber performance.

In Chapter 4, the effect of compression is examined by measuring the sound absorption and bulk properties of samples as they are gradually compressed. Relationships between the flow resistivity and compression ratio are developed for fibers and foams.

Chapter 5 summarizes the work in this thesis. The major contributions are summarized and possible future work is suggested.

.

Chapter 2 Bulk Properties Measurement and Prediction

2.1 Introduction

This chapter details the different approaches that can be used to assess the bulk properties of sound absorbing materials. The bulk properties include the characteristic impedance (Z_c) and complex wave number (k_c). Once known, the sound absorption and surface impedance of any thickness of sound absorber can be determined. Moreover, the sound absorption and the surface impedance of layered materials can be identified. The bulk properties can be used directly in finite and boundary element models. Surface impedance is often used as a boundary condition to model thin materials and sound absorption is used in statistical energy analysis models.

The bulk properties may be assessed in a number of different ways. They may be measured directly using an impedance tube using the setup described in ASTM E2611 (2010). ASTM E2611 describes the two-load method (Song and Bolton, 2000) though the two-source method (Tao, 2003) uses the same algorithm and may be used as well. The two-load method is generally preferred due to measurement ease. For the two-load method two measurements are performed with different terminations. Other alternatives are the two-cavity method (Utsuno, 1989) which specifies two different cavity depths for the two acoustic loads and the three-microphone method (Salissou and Panneton, 2010) which requires no modification of the acoustic load but instead an extra measurement at the end of the tube. Each of these direct measurement approaches are detailed in the sections that follow.

.

Indirect measurement of the bulk properties can be accomplished by measuring the flow resistivity directly via ASTM C522 (2009). Alternatively, the flow resistivity can be determined by first measuring the sound absorption using ASTM E1050 (2012) and then using a curve fit to identify an effective flow resistivity based on one of several empirical models.

Each of the aforementioned measurement approaches and associated algorithms will be detailed in this section. Transfer matrix theory will be introduced first since this serves as the basis for much of what follows. After which, direct measurement approaches will be summarized followed by the indirect approaches.

2.2 Transfer Matrix Method

Acoustic plane wave propagation can be assumed so long as the cross-section dimension of a circular duct or pipe is less than $c/1.71d$ (Eriksson, 1980), where c is the speed of sound (343 m/s in air) and d is the diameter of the duct or pipe. As shown in Figure 2.1, the sound pressure can be expressed as the superposition of a forward traveling and reflected wave in a duct. Accordingly, the total sound pressure and particle velocity at any point in the duct or pipe can be expressed as:

$$p(x) = P_{+}e^{-jkx} + P_{-}e^{jkx} \tag{2.1}$$

and

$$u(x) = \frac{-1}{jk\rho_0 c}\frac{dp}{dx} \tag{2.2}$$

respectively where k is the wavenumber, and ρ_0 is the air density. The wave number is expressed as $k = \omega/c$ where ω is the angular frequency. In that case,

the sound pressure and particle velocity on one side of the sample can be related to that on the other side via a transfer matrix.

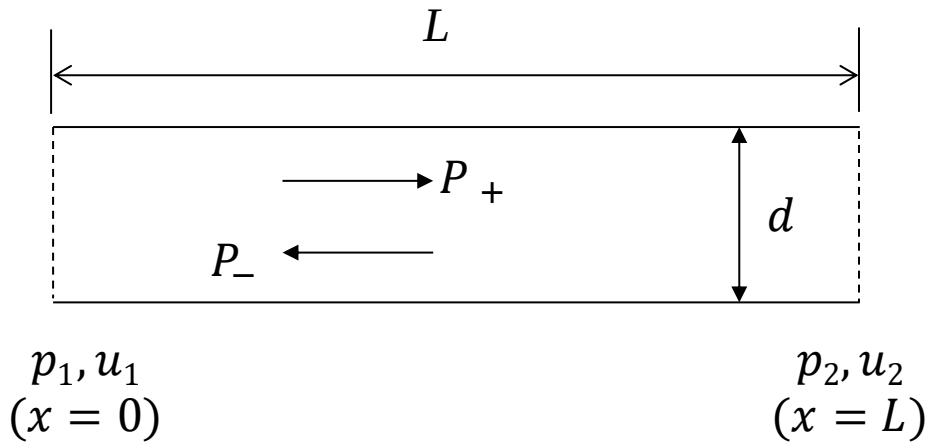

Figure 2.1 Schematic illustrating plane wave propagation in a circular duct or pipe.

The sound pressure and particle velocity at $x = 0$ and $x = L$ can be expressed as:

$$p(0) = p_1 = P_+ + P_- \qquad p(L) = p_2 = P_+ e^{-jkL} + P_- e^{jkL}$$
$$u(0) = u_1 = \frac{P_+ - P_-}{\rho_0 c} \qquad u(L) = u_2 = \frac{P_+ e^{-jkL} - P_- e^{jkL}}{\rho_0 c} \tag{2.3}$$

After some simplification, the equations can be expressed in a form:

$$\begin{Bmatrix} p_1 \\ u_1 \end{Bmatrix} = \begin{bmatrix} T_{11} & T_{12} \\ T_{21} & T_{22} \end{bmatrix} \begin{Bmatrix} p_2 \\ u_2 \end{Bmatrix} \tag{2.4}$$

relating the sound pressure and particle velocity on one side to the other. By manipulating Equation 2.3, the transfer matrix for a straight duct is expressed as:

$$\begin{Bmatrix} p_1 \\ u_1 \end{Bmatrix} = \begin{bmatrix} \cos(kL) & j\rho_0 c \sin(kL) \\ j\dfrac{\sin(kL)}{\rho_0 c} & \cos(kL) \end{bmatrix} \begin{Bmatrix} p_2 \\ u_2 \end{Bmatrix} \tag{2.5}$$

where p_1, u_1 and p_2, u_2 are the respective sound pressures and particle velocities on either side of the sample, and L is the length of the duct or pipe.

Plane wave theory can be extended to describe the acoustic performance of porous materials in the duct or pipe. The relationship between the sound pressure and particle velocity can be expressed as:

$$p_1 = p_2 \cos(k_c l) + u_2 \, jZ_c \sin(k_c l) \tag{2.6}$$

and

$$u_1 = jp_2 \frac{\sin(k_c l)}{Z_c} + u_2 \cos(k_c l) \tag{2.7}$$

where Z_c is the characteristic impedance, k_c is the complex wavenumber and l is the thickness of the porous material. Then the transfer matrix will be:

$$\begin{Bmatrix} p_1 \\ u_1 \end{Bmatrix} = \begin{bmatrix} \cos(k_c l) & jZ_c \sin(k_c l) \\ j\dfrac{\sin(k_c l)}{Z_c} & \cos(k_c l) \end{bmatrix} \begin{Bmatrix} p_2 \\ u_2 \end{Bmatrix} \tag{2.8}$$

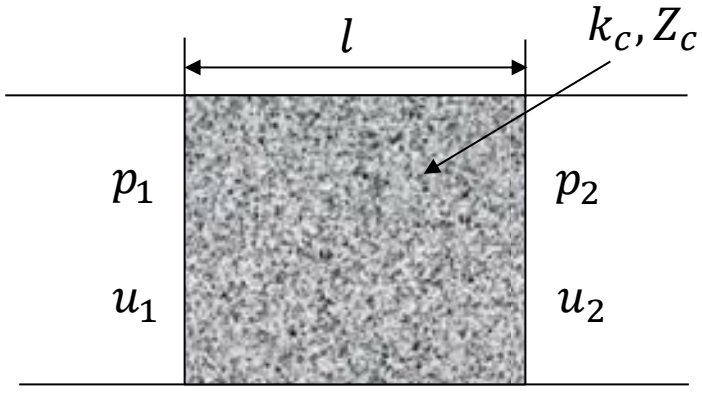

Figure 2.2 Porous material in the duct or pipe.

The sound absorption can be calculated in the following way. If we assume plane wave propagation and that the sound absorber is backed by a rigid wall, the particle

velocity on the right side of the sample will be zero. From Equation 2.8, it can be seen that the impedance can be expressed as:

$$Z = \frac{p_1}{u_1} = \frac{T_{11}}{T_{21}} = -Z_c \coth(k_c l) \tag{2.9}$$

A reflection coefficient, which is complex, is defined as:

$$R = \frac{Z - \rho_0 c}{Z + \rho_0 c} \tag{2.10}$$

and the normal incidence sound absorption is expressed as:

$$\alpha = 1 - |R|^2 \tag{2.11}$$

The transmission loss, which characterizes how easily sound propagates through a material if it is used as a barrier, is also of interest. The transmission loss is defined as the difference between the incident and transmitted power (assuming an anechoic termination) in decibels (dB). Figure 2.3 illustrates the metric.

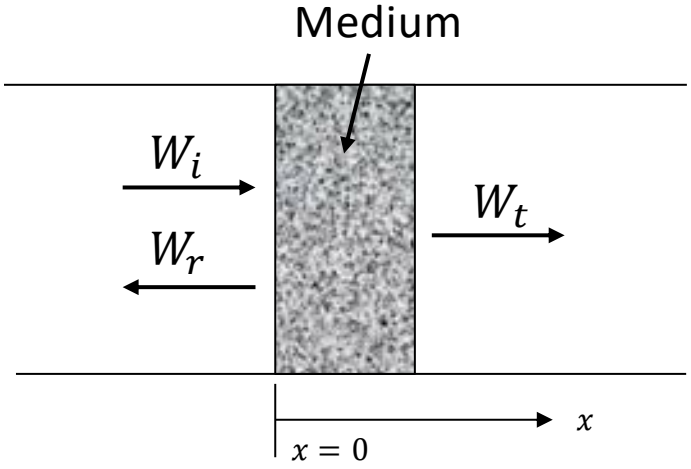

Figure 2.3 Illustration of transmission loss.

The transmission loss can be expressed as:

$$TL = 10 \log_{10} \frac{W_i}{W_t} \tag{2.12}$$

where W_i is the incident sound power, W_r is the reflected sound power and W_t is the transmitted sound power. If the transfer matrix for a material of given thickness is known, the transmission loss (Song and Bolton, 2001, Wallin et al., 2010) can be expressed as:

$$TL = 20 \log_{10} \left| T_{11} + \frac{T_{12}}{\rho_0 c} + \rho_o c T_{21} + \frac{T_{22}}{2} \right| \tag{2.13}$$

2.2.1 Mass Layer Transfer Impedance

Foil and mylar covers are often used to cover sound absorbing materials. These covers improve the low frequency performance but also prevent the materials from getting soaked with oil or other fluids. A thin cover can be modeled as a simple mass. Hence, it can be assumed that the particle velocity is constant on both sides of the cover. The pressure drop from one side to the other is largely dependent on the mass of the sample.

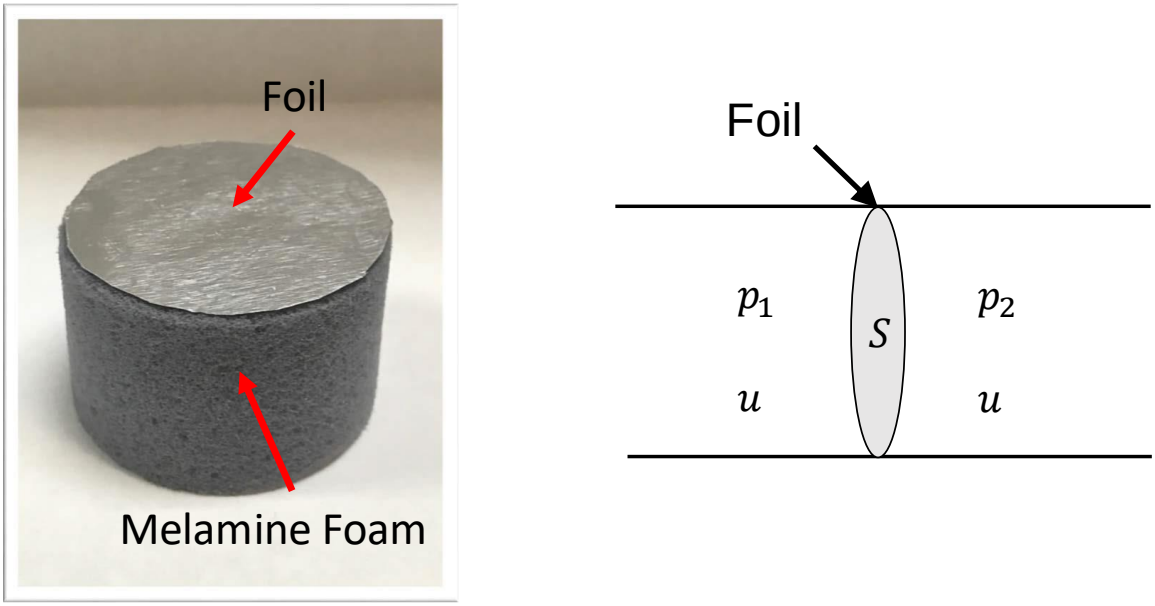

a) b)

Figure 2.4 a) Foil cover on the melamine foam. b) Foil cover in a circular duct or pipe.

From equilibrium, it can be seen that:

$$j\omega muS = p_1 - p_2 \tag{2.14}$$

and a transfer impedance can be expressed as:

$$Z_{tr} = \frac{p_1 - p_2}{u} = j\omega mS \tag{2.15}$$

where $\omega = 2\pi f$ is the angular frequency, m is the mass of the foil and S is the surface area of the foil. The transfer matrix for the mass layer can be expressed as:

$$[T] = \begin{bmatrix} 1 & Z_{tr} \\ 0 & 1 \end{bmatrix} \tag{2.16}$$

where Z_{tr} is as defined in Equation (2.15).

.

2.2.2 Multi-layer Absorber Sound Absorption Coefficient Prediction

Once the flow resistivity for a material is known, the sound absorption or impedance can be determined for any thickness. In addition, the sound absorption of layered materials can be calculated. A schematic of a layered sound absorber is shown in Figure 2.5.

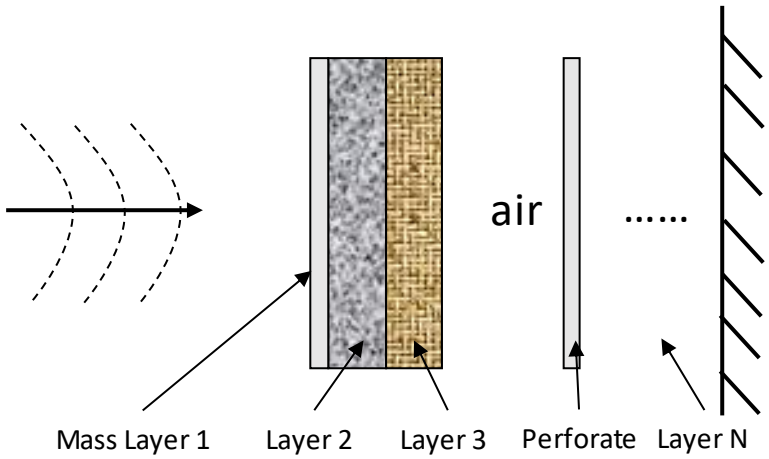

Figure 2.5 Schematic of a layered sound absorber.

The thickness of each layer is easily varied by just varying l in Equation 2.8. The transfer matrix for the individual elements can be multiplied together in order to determine the transfer matrix from the front to the rear of the sample. Hence,

$$[T_{total}] = [T_1][T_2][T_3] \dots [T_N] = \begin{bmatrix} T_{11} & T_{12} \\ T_{21} & T_{22} \end{bmatrix} \tag{2.17}$$

where $[T_i]$ are the individual transfer matrices for the different sound absorbing material layers assuming there are N layers. The impedance can be determined using Equation 2.9. Once the impedance is known, the sound reflection coefficient (R) and sound absorption (α) can be determined by Equations 2.10 and 2.11.

2.3 Instrumentation

Regardless of the measurement approach, the measurement process consists of two parts: data acquisition and data processing. Data acquisition requires an impedance tube equipped with microphones, data acquisition system (DAQ), and computer. There are a number of commercial systems available. The system used for the research in this thesis is the Spectronics impedance tube and the Siemens SCADAS data acquisition system with Siemens Test.Lab software. The microphones used are PCB 1/2-inch microphones (377B11). After the data is acquired, Matlab was used to process the measurement data.

2.3.1 ASTM E1050 Two-Microphone Method

The two-microphone method is used for determining the sound absorption, reflection coefficient, and surface impedance of a sample. Though it is not used for direct determination of the bulk properties, it is covered first because it is the simplest measurement approach and it will be referred to later on. Figure 2.6 shows the measurement setup for the two microphone method. The schematic shows the impedance tube containing the sound absorptive material specimen and microphones upstream of the sample. Figure 2.7 shows a photograph of a typical impedance tube.

.

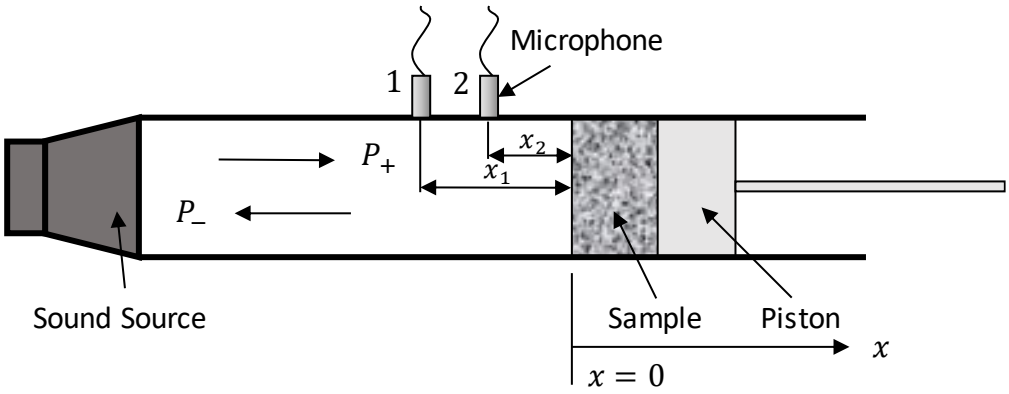

Figure 2.6 Schematic diagram of two-microphone method apparatus.

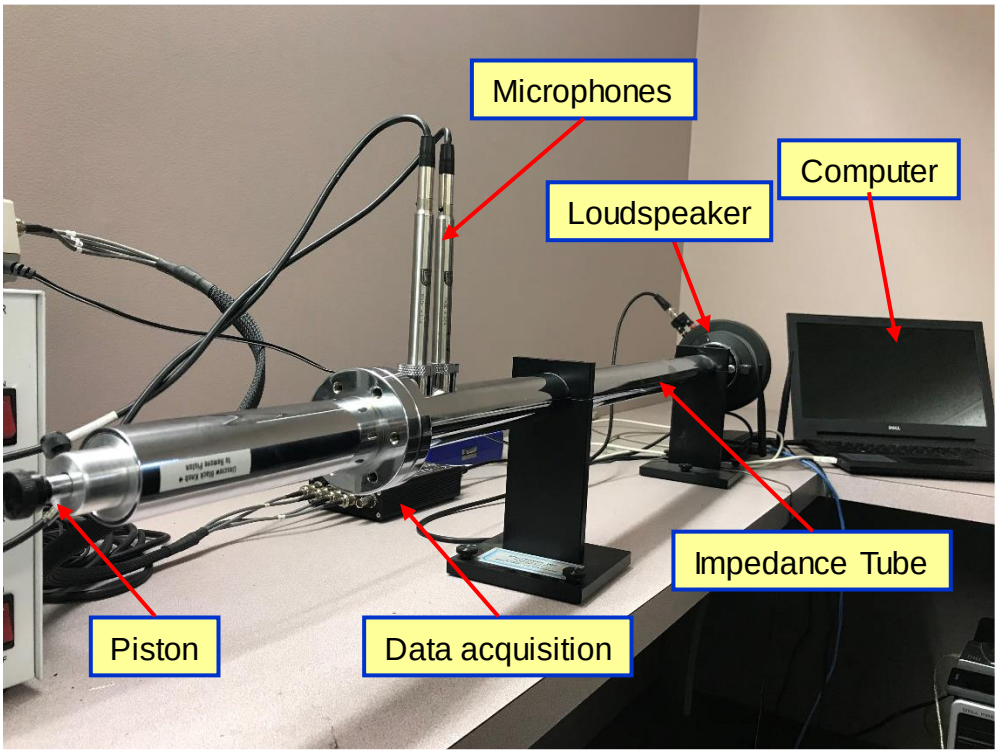

Figure 2.7 Photograph of a typical impedance tube.

The test sample is placed at one end of the impedance tube with a piston pushed flush against the sample. The sound source, a compression driver loudspeaker (JBL 2426H) is at the other and there is no gap between the sample and the piston. A broadband random or white noise signal is applied to the speaker and the transfer function between the two microphones is measured.

Based on plane wave theory which assumes that the sound pressure is constant across the cross-section of the tube, the total sound pressure at any point in the impedance tube can be expressed as:

$$p(x) = P_{+}e^{-jkx} + P_{-}e^{jkx} \tag{2.18}$$

where P_{+} and P_{-} are the incident and reflected complex pressure amplitudes respectively. k is the wavenumber for air which can be expressed as ω/c where ω is the angular frequency and c is the speed of sound (343 m/s for air at room temperature). The transfer function between microphones 1 and 2 may be expressed as:

$$H_{12} = \frac{p(x_2)}{p(x_1)} = \frac{P_{+}e^{-jkx_2} + P_{-}e^{jkx_2}}{P_{+}e^{-jkx_1} + P_{-}e^{jkx_1}} = \frac{e^{-jkx_2} + Re^{jkx_2}}{e^{-jkx_1} + Re^{jkx_1}} \tag{2.19}$$

where $R = P_{-}/P_{+}$ is the sound pressure reflection coefficient of the material and the positions for x_1 and x_2 are indicated in Figure 2.6.

The reflection coefficient can be solved for and expressed as

$$R = \frac{e^{-jkx_2} - H_{12}e^{-jkx_1}}{H_{12}e^{jkx_1} - e^{jkx_2}} \tag{2.20}$$

Normal incidence sound absorption coefficient can be determined by Equation 2.11.

2.3.2 ASTM E2611 Two-Load Method

The bulk properties can be measured directly using a more complicated measurement process called the two-load method (Song and Bolton, 2000) which has been standardized in ASTM E2611 (2010). The acoustic load is varied twice by changing the termination of the impedance tube. Figure 2.8 shows the

.

measurement setup for the two-load method. Note that two microphones are placed downstream of the sample.

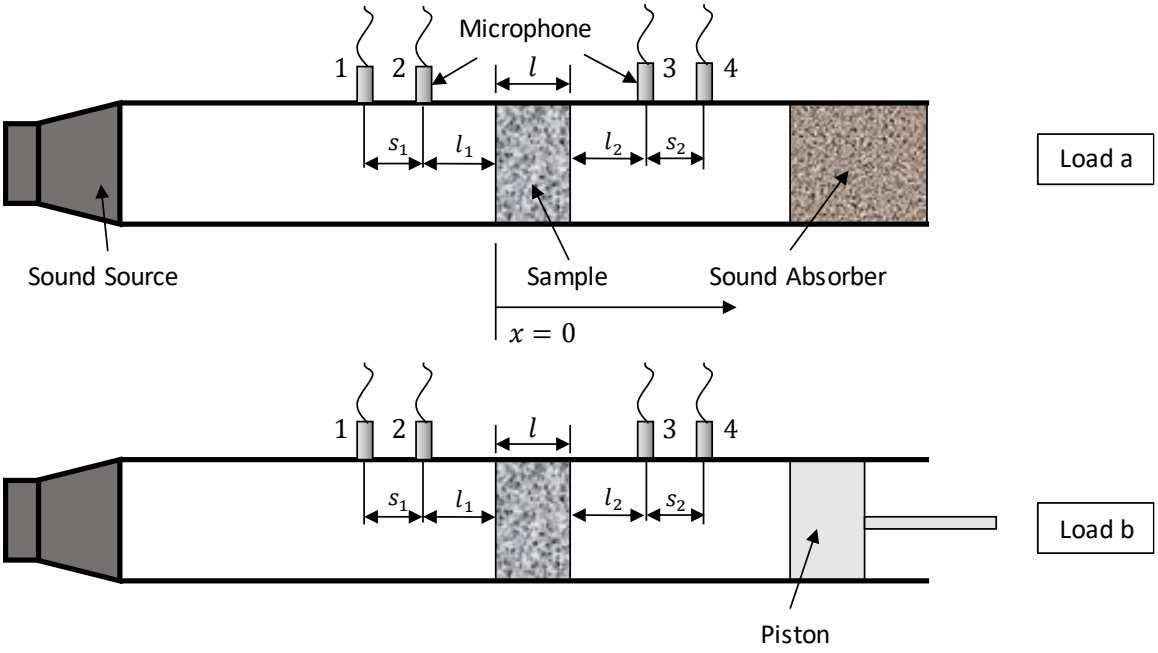

Figure 2.8 Schematic diagram of two-load method apparatus.

The test sample is placed between microphones 2 and 3 and the sound source is positioned at the left end of the impedance tube. A broadband random excitation signal is applied to the speaker and transfer functions are measured in between a reference microphone and the other three microphones. For the measurements detailed in this thesis, the microphone reference is set to microphone 1 though any of the other microphones could be selected. The acoustic load is varied twice. In this work, loads a and b were with sound absorption on one end and with the impedance tube capped respectively. Any choice of acoustic loads is appropriate so long as they are sufficiently different from one another.

The transfer matrix relates the acoustic pressure and particle velocity on the front and back surface of the sample. For each load case, the acoustic wave field can be decomposed to forward and backward traveling waves on either side of the sample as shown in Figure 2.1. The wave amplitudes can be expressed as:

$$P_1 = j\frac{e^{-jkl_1} - H_{21}e^{-jk(l_1+s_1)}}{2\sin ks_1} \qquad P_2 = j\frac{H_{21}e^{jk(l_1+s_1)} - e^{jkl_1}}{2\sin ks_1}$$
$$P_3 = j\frac{H_{31}e^{jk(l_2+s_2)} - H_{41}e^{jkl_2}}{2\sin ks_2} \quad P_4 = j\frac{H_{41}e^{-jkl_2} - H_{31}e^{-jk(l_2+s_2)}}{2\sin ks_2} \tag{2.21}$$

where H_{21}, H_{31} and H_{41} are the transfer functions between microphones 2, 3 and 4 and microphone 1 with microphone 1 as a reference, s_1 and s_2 are the centerline distances between microphones 1 and 2 and between 3 and 4 respectively. l_1 and l_2 are the distances from microphone 2 to the sample and from the sample to microphone 3 respectively. The sound pressure and particle velocity at each face of the sample (at $x = 0$ and at $x = l$) can be expressed as:

$$p_0 = P_1 + P_2 \qquad p_d = P_3e^{-jkl} + P_4e^{jkl}$$
$$u_0 = (P_1 - P_2)/\rho_0 c \qquad u_d = \left(P_3e^{-jkl} - P_4e^{jkl}\right)/\rho_0 c \tag{2.22}$$

The sound pressures and the particle velocities can be calculated on each side of the sample for acoustic loads *a* and *b*. The transfer matrix can be expressed as:

$$[T] = \begin{bmatrix} T_{11} & T_{12} \\ T_{21} & T_{22} \end{bmatrix} = \begin{bmatrix} \dfrac{p_{0a}u_{lb} - p_{0b}u_{la}}{p_{la}u_{lb} - p_{lb}u_{la}} & \dfrac{p_{0b}u_{la} - p_{0a}u_{lb}}{p_{la}u_{lb} - p_{lb}u_{la}} \\ \dfrac{p_{0a}u_{lb} - p_{0b}u_{la}}{p_{la}u_{lb} - p_{lb}u_{la}} & \dfrac{p_{la}u_{0b} - p_{lb}u_{0a}}{p_{la}u_{lb} - p_{lb}u_{la}} \end{bmatrix} \tag{2.23}$$

where the first footnote indicates the position (at $x = 0$ or at $x = l$), and the second indicates the termination (load a or load b). The transmission loss can be determined by Equation 2.13.

From the four pole matrix for a sound absorbing material (Equation 2.23), the characteristic impedance (Z_c) and complex wavenumber (k_c) can be solved for in terms of individual transfer matrix terms and expressed as:

$$Z_c = \sqrt{T_{12}/T_{21}} \tag{2.24}$$

and

$$k_c = \frac{1}{d}\cos^{-1}(T_{11}) \tag{2.25}$$

respectively.

2.3.3 Three-Microphone Method

The three microphone method developed by Iwase et al. (1998) eliminates the need for another acoustic load. It assumes that the sample is homogeneous. If so, an additional microphone placed behind a rigid backed sample will be sufficient to determine the bulk properties. As can be seen in Figure 2.9, the measurement setup is identical to ASTM E1050 (2012) except an additional microphone is placed at the end of the impedance tube. The advantage of the method is that a single load is sufficient.

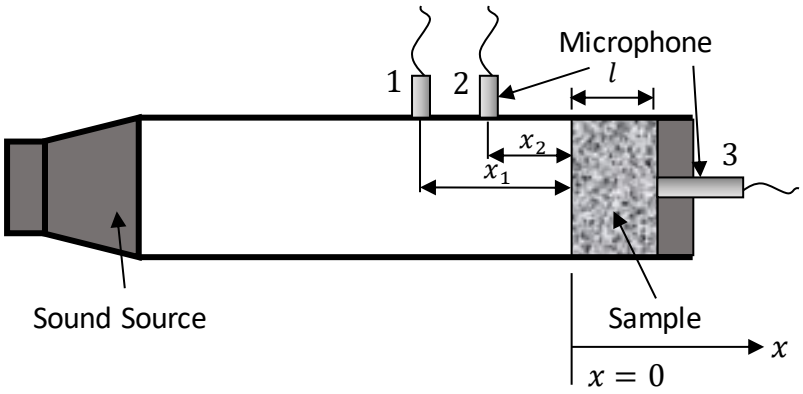

Figure 2.9 Schematic diagram of three-microphone method apparatus.

The transfer functions between microphones 1 and 2 (H_{12}) and microphones 2 and 3 (H_{23}) are measured (Equation 2.19). The reflection coefficient can be determined via Equation 2.20. The complex wavenumber (k_c) and characteristic impedance (Z_c) for the material can then be found using:

$$k_c = \frac{1}{l}\cos^{-1}\left(\frac{1+R}{e^{jkx_2}+Re^{-jkx_2}}H_{23}\right) \tag{2.26}$$

and

$$Z_c = j\rho_0 c\frac{1+R}{1-R}\tan(k_c l) \tag{2.27}$$

respectively.

2.3.4 Two-Cavity Method

The bulk properties of sound absorbing materials can also be measured using the two-cavity method (Utsuno, 1989). The test setup is similar to ASTM E1050 (2012) except an air space of known length is introduced behind the sample. The length is varied twice which effectively varies the acoustic load. Since the acoustic load is well understood and characterized, there is no need to make measurements behind the sample. A schematic of the test setup is shown in Figure. 2.10.

.

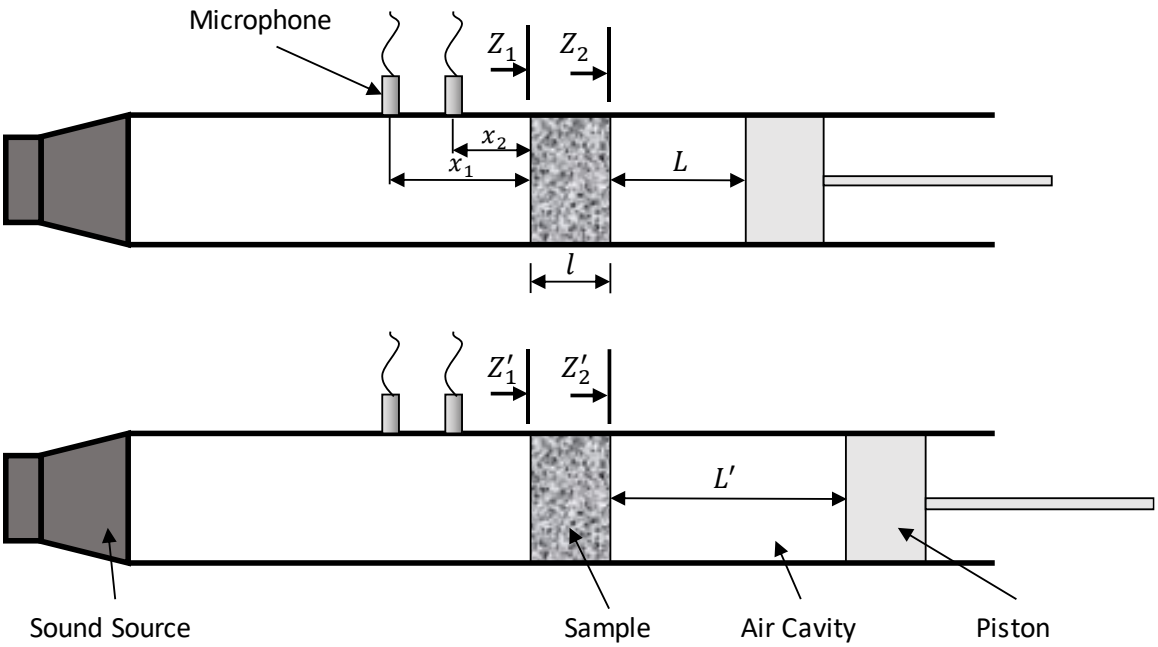

Figure 2.10 Schematic diagram of two-cavity method apparatus.

The transfer functions between microphones 1 and 2 (H_{12}) with two different cavity lengths are measured. The impedance (Z_1) is measured using ASTM E1050 (2012) at the surface of the sample. The impedance behind the sample is calculated easily using Equation 2.9 where the wavenumber and characteristic impedance for air are used. The air cavity depth is then adjusted and Z_1' measured again. The bulk properties can then be calculated using the two measured and two known air cavity impedances. The characteristic impedance and complex wavenumber are expressed as:

$$Z_c = \sqrt{\frac{Z_1 Z_1'(Z_2 - Z_2') - Z_2 Z_2'(Z_1 - Z_1')}{(Z_2 - Z_2') - (Z_1 - Z_1')}} \tag{2.28}$$

and

$$k_c = \frac{1}{2jl} \ln\left(\frac{Z_1 + Z_c}{Z_1 - Z_c}\frac{Z_2 - Z_c}{Z_2 + Z_c}\right) \tag{2.29}$$

respectively.

The impedances for the known cavity depths can be expressed as:

$$Z_1 = -jZ_{air}\cot(kL) \tag{2.30}$$

and

$$Z_1' = -jZ_{air}\cot(kL') \tag{2.31}$$

respectively where k is the wavenumber of air and Z_{air} is the characteristic impedance of air.

2.3.5 ASTM C522 Flow Resistivity Measurement

The bulk properties may also be determined indirectly from the flow resistivity. The instrumentation for the test is detailed in ASTM C522 (2009). A photograph of the measurement setup at the University of Kentucky is shown in Figure 2.11a and a schematic of the test is shown in Figure 2.11b. Notice that the static pressure drop (Δp_S) is measured via a manometer and the flow speed using a flow meter. The flow resistivity (σ) is defined as the static pressure drop (Δp_S) divided by the flow speed (u_S) and is expressed as:

$$\sigma = \frac{\Delta p_S}{u_S l} \tag{2.32}$$

where l is the thickness of the sample.

.

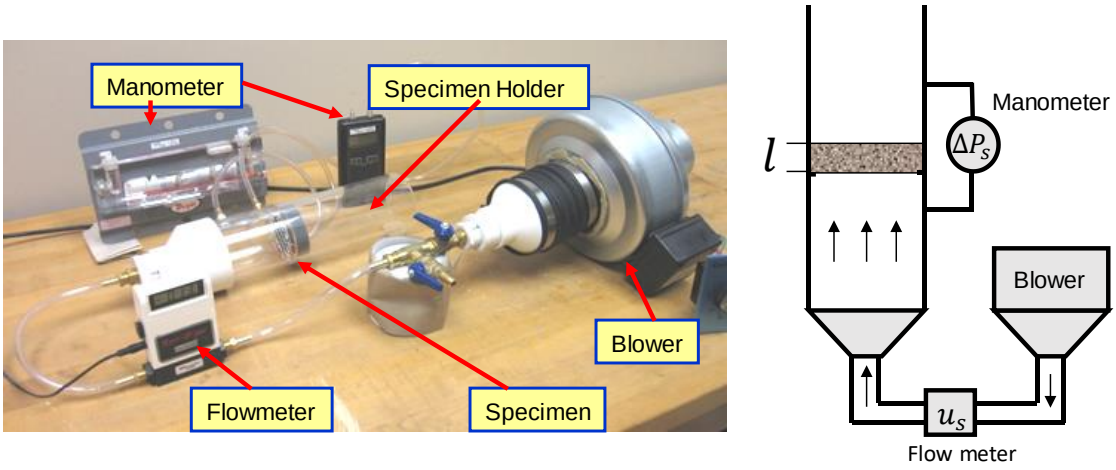

a) b)

Figure 2.11 a) Photograph of the measurement setup at the University of Kentucky. b) Schematic diagram of flow resistivity measurement apparatus

2.4 Empirical Model Based On Flow Resistivity

Several empirical models have been developed which relate the bulk properties to the measured flow resistivity. The models are identical in form but vary in the constants used. The input variable to the models is the non-dimensional parameter X which can be defined as

$$X = \rho f / \sigma \tag{2.33}$$

where ρ is the mass density of the fluid (e.g., normally air), and f is the frequency in Hz. Once the flow resistivity is established, the characteristic impedance (Z_c) and complex wavenumber (k_c) for the material can be expressed as

$$Z_c = Z_0[1 + C_1 X^{-C_2} - jC_3 X^{-C_4}] \tag{2.34}$$

$$k_c = k_0[1 + C_5 X^{-C_6} - jC_7 X^{-C_8}] \tag{2.35}$$

where k_0 and Z_0 are the wavenumber and characteristic impedance for air respectively. C_1, C_2, C_3, C_4, C_5, C_6, C_7, and C_8 are empirically developed constants.

Models for fiber include those of Delaney and Bazley (1970), Miki (1990), and Mechel (1988). Garai and Pompoli (2005) developed an empirical equation for polyester fiber. In a similar manner, Dunn and Davern (1986) and Wu (1988) developed equations for polyurethane and plastic foams respectively. Bies and Hansen (1980) compiled these empirical constants into a table and a more complete version of the table is shown in Table 2.1. The empirical models used in this thesis research are those of Mechel (1988) and Wu (1988) for fibers and foams respectively.

Table 2.1 Parameters for Empirical Model

Material type reference	C_1	C_2	C_3	C_4	C_5	C_6	C_7	C_8
Rockwool/fiberglass								
Delaney and Bazley (1970)	0.0571	0.754	0.087	0.732	0.0978	0.700	0.189	0.595
Rockwool/fiberglass								
Miki (1989)	0.070	0.632	0.107	0.632	0.109	0.618	0.160	0.618
Polyester								
Garai and Pompoli (2005)	0.078	0.623	0.074	0.660	0.159	0.571	0.121	0.530
Polyurethane foam of low flow resistivity								
Dunn and Davern (1986)	0.114	0.369	0.0985	0.758	0.168	0.715	0.136	0.491
Porous plastic foams of medium flow resistivity								
Wu (1988)	0.209	0.548	0.105	0.607	0.188	0.554	0.163	0.592
Fiber								
Mechel (2002) (X<0.025)	0.081	0.699	0.191	0.556	0.136	0.641	0.322	0.502
(X>0.025)	0.0563	0.725	0.127	0.655	0.103	0.716	0.179	0.663

The specific acoustic impedance of a sound absorber having thickness l can be determined by using Equation 2.9. It follows that the reflection coefficient (R) and sound absorption (α) can then be determined by using Equation 2.10 and Equation 2.11 respectively.

.

2.4.1 Least Squares Data Fitting

Rather than measuring the flow resistivity, several researchers have recommended measurement of material properties in an impedance tube and then the use of a least squares curve fit to minimize the errors between the measured properties and those calculated using phenomenological or empirical equations. Typically, the flow resistivity or other properties are identified. For example, Braccesi and Bracciali (1997) minimized the error in the reflection coefficient to determine the flow resistivity and structure factor. Zieliński (2005) used the measured impedance and curve fit to the properties specific to the Johnson-Champoux-Allard (JCA) model (Johnson, 1987, Champoux, 1991, Allard, 1993). Simón et al. (2006) measured the sound absorption coefficient and curve fit to the models of Delaney and Bazley (1970), Mechel (1988), and Allard and Champoux (1988). The approach used by Simón et al. (2006) is adopted here but some improvements are made.

2.4.2 Empirical Model Comparison

There are 6 different empirical models in table 2.1, 4 for fibrous materials and 2 for porous foam materials. As a demonstration, each of the empirical models are plotted for a flow resistivity of 2400 rayls/m with thickness of 40 mm in Figure 2.12. It can be seen that each of the curves has a similar shape. Only the lesser used models of Garai and Pompoli (2005) and Dunn and Davern (1986) differ greatly from the others. The measured sound absorption of a fiber with that measured flow resistivity is included for reference.

.

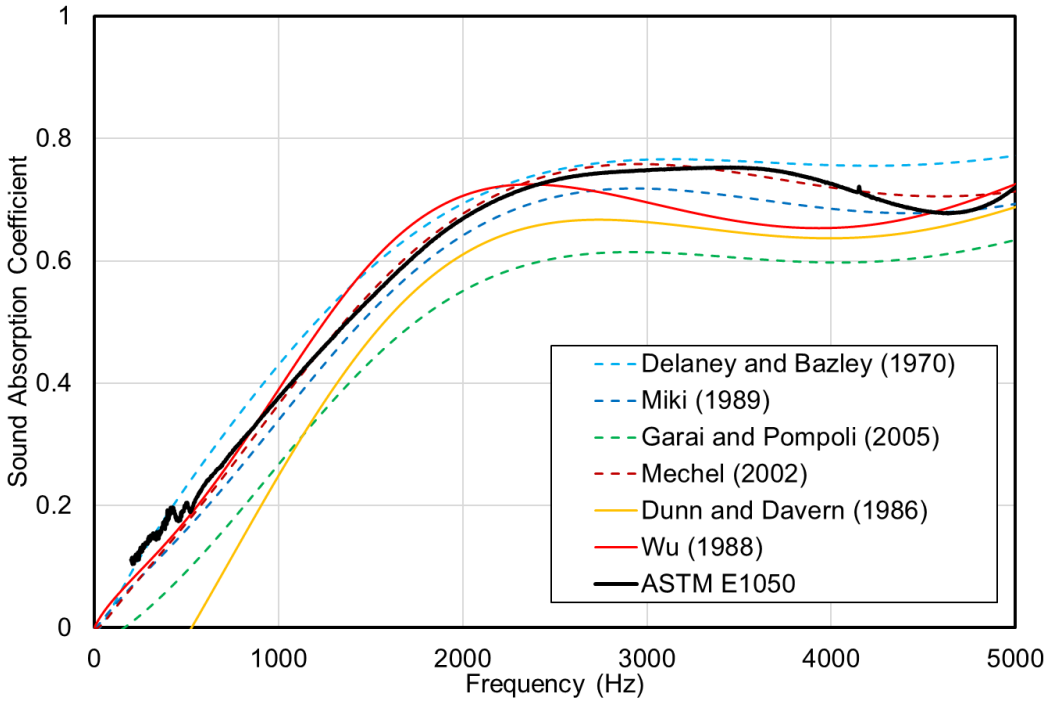

Figure 2.12 40 mm polyester fiber flow resistivity comparison (2400 rayls/m)

Figures 2.13 and 2.14 show similar comparisons for a flow resistivity of 8400 rayls/m with thickness of 24 mm and a flow resistivity of 1930 rayls/m with thickness of 28.5 mm. Similar conclusions are reached.

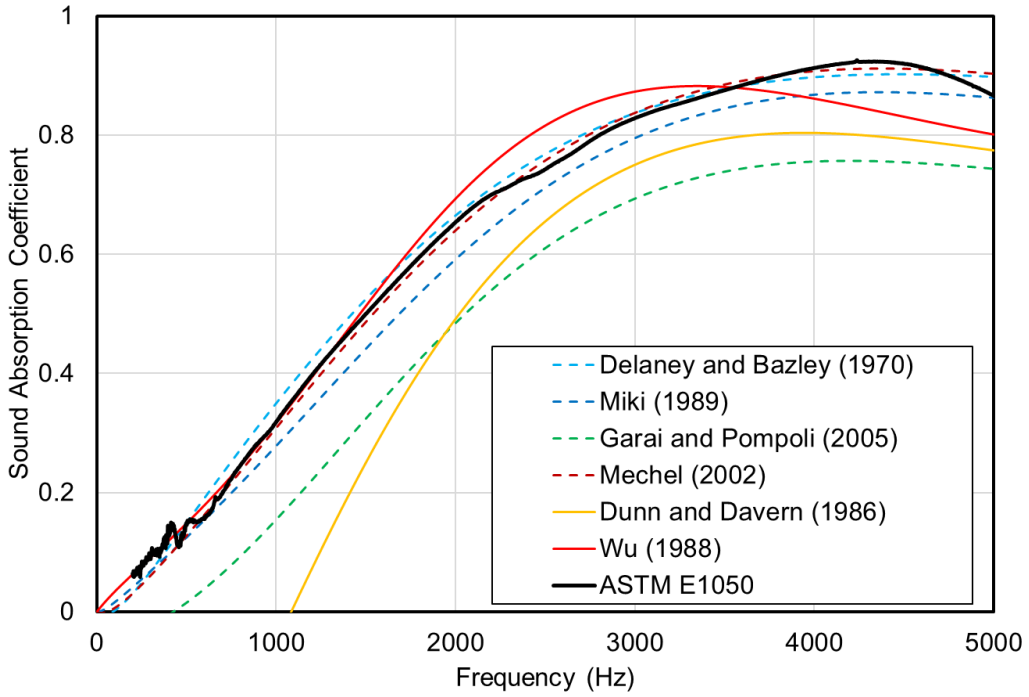

Figure 2.13 24 mm melamine foam flow resistivity comparison (8400 rayls/m)

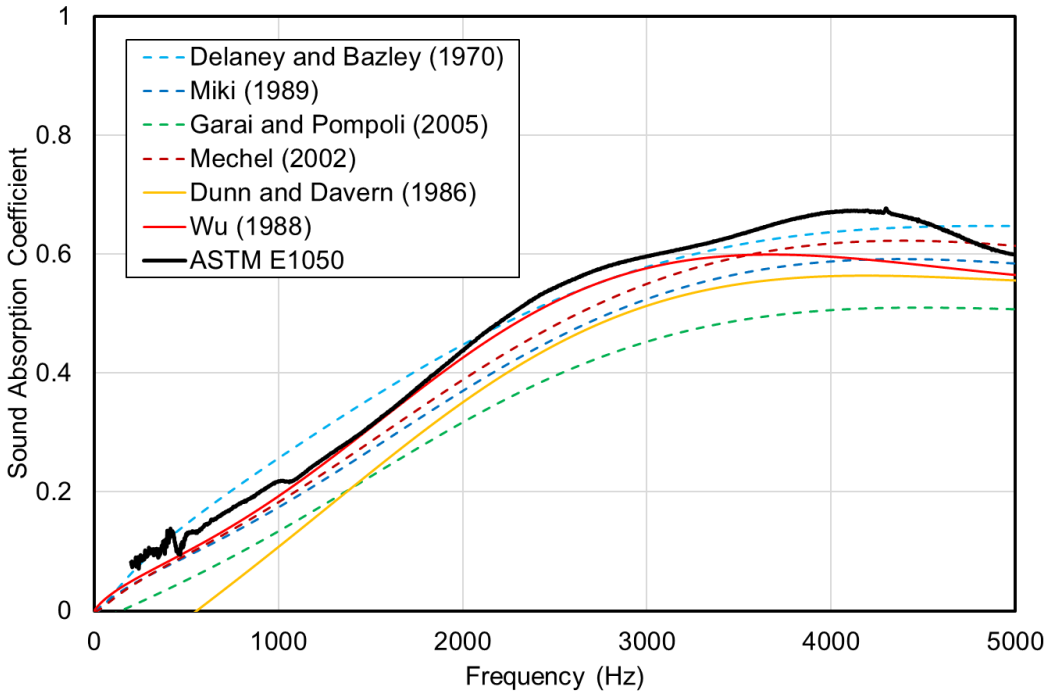

Figure 2.14 28.5 mm polyurethane foam flow resistivity comparison (1930 rayls/m)

Alternatively, the sound absorption can be measured using ASTM E1050 (2012) in an impedance tube and then an optimal flow resistivity can be curve fitted using any of the empirical models. This was checked using both a 40 mm polyester fiber and a 24 mm melamine foam. The flow resistivity was determined by curve fitting to each of the 6 empirical models. It can be seen that there are some differences between the empirical models. If the models of Garai and Pompoli (2005) and Dunn and Davern (1986) are ignored, there is little difference between the other four empirical models and they all agree well with the measurement. Predicted sound absorptions based on curve fits to each empirical model are shown in Figure 2.15 and 2.16 for a polyester fiber and a melamine foam. The fitted flow resistivities are shown in Table 2.2.

Table 2.2 Fitted flow resistivities with different empirical models

Empirical Model	Polyester Fiber (rayls/m)	Melamine Foam (rayls/m)
Delaney and Bazley (1970)	2104	7601
Miki (1989)	2784	9825
Garai and Pompoli (2005)	4470	15658
Mechel (2002)	2387	8190
Dunn and Davern (1986)	3443	13021
Wu (1988)	2438	7238

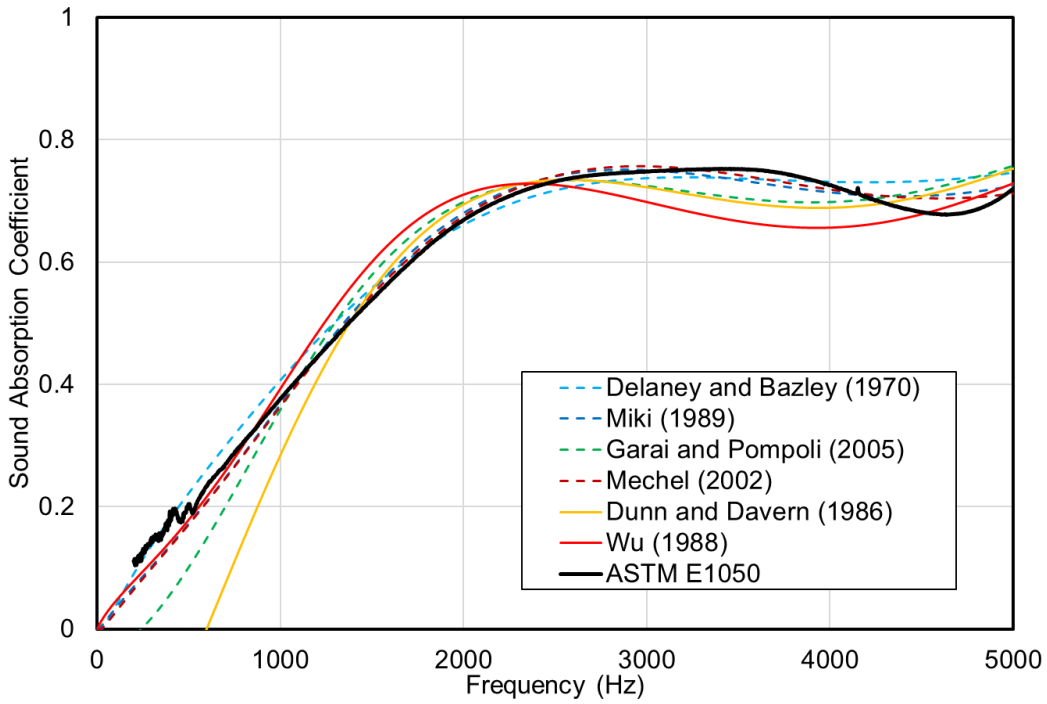

Figure 2.15 40 mm Polyester fiber curve fit comparison.

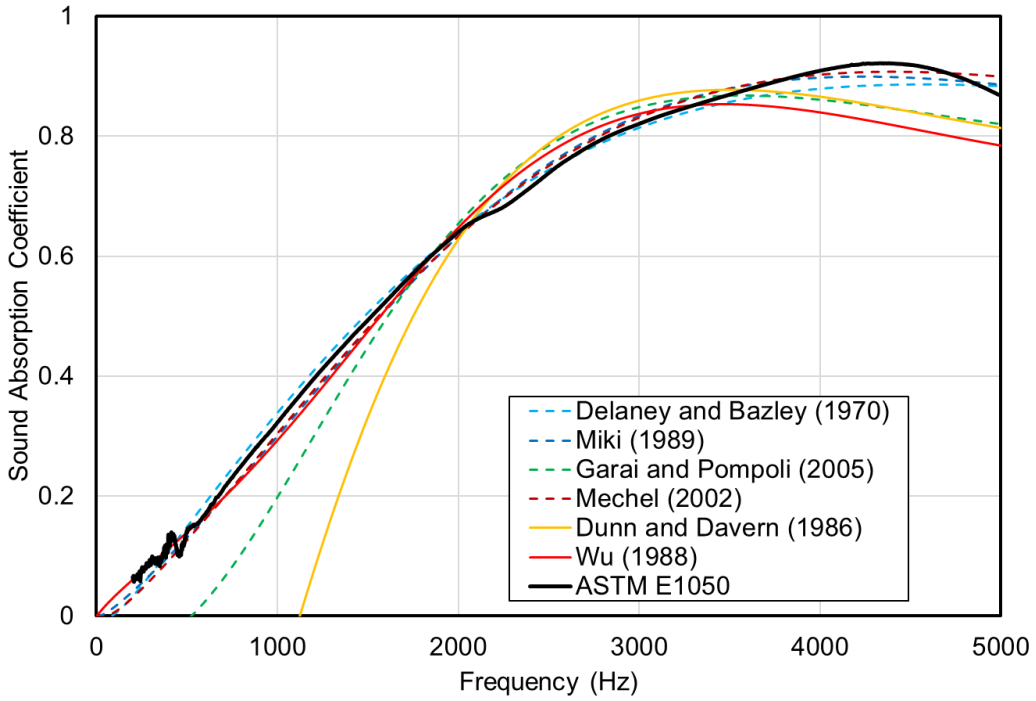

Figure 2.16 24 mm Melamine curve fit comparison.

2.5 Conclusions

In this chapter, several methods to determine the bulk properties have been detailed. The advantages and disadvantages of each method are compared. Direct measurement approaches include the two-load, two-cavity, and three-microphone approaches. Each of the methods are similar and should provide identical results.

Indirect methods to determine the bulk properties have also been detailed. These include methods to measure the flow resistivity and identify bulk properties based on empirical models. There are also phenomenological models but these require measurement or curve fitting to determine 5 variables also known as Biot parameters. For the work in this research, the simpler empirical models are used.

.

Chapter 3 Rudimentary Materials Database

Empirical models based on flow resistivity are commonly used to characterize the complex wavenumber and characteristic impedance of common sound absorbing materials such as fibers and foams. Airflow resistance is measured using ASTM C522 (2009) and then plugged into empirical models that have been developed for fibers and plastic foams. In this work, the sound absorption coefficient of sound absorbing materials is measured in an impedance tube using ASTM E1050 (2012). The measured data is then used to determine the flow resistivity via a least squares curve fit and the flow resistivity is selected to insure the best fit. Different fitting schemes are examined and the calculated flow resistivity is generally similar regardless of the scheme. Results for several commonly used foams and fibers are tabulated to form a rudimentary materials database. The database is then used in conjunction with transfer matrix theory to predict the sound absorption of layered absorbers with good agreement to measurement.

3.1 Introduction

Interior noise is frequently reduced by the liberal application of sound absorbing materials. Applications include but are not limited to automobile and heavy equipment cabins, under hood applications, partial enclosures, and HVAC ductwork. There are a number of different methods for characterizing sound absorbing materials. Material manufacturers prefer using reverberation room measurements to determine the diffuse field sound absorption coefficient. Though useful for room acoustics applications, the diffuse field sound absorption is not suitable as an input for most numerical models.

.

Instead, analysts prefer to use specific acoustic impedance or bulk properties (complex wavenumber and complex characteristic impedance), which are obtained via impedance tube measurements. ASTM E1050 (2012) is used to determine the normal incident sound absorption and specific impedance while the more complicated two-load method detailed in ASTM E2611 (2010) is commonly used to determine the bulk properties. The specific acoustic impedance is used directly in simulation models as a boundary condition whereas the bulk properties are used to model the sound absorber itself. Bulk properties can be used to model any porous sound absorber and are especially useful if the sound absorber is thick.

However, impedance tube approaches are difficult for those who are not skilled practitioners (Stanley, 2012). Samples should be precisely the size of the impedance tube, but correctly sized samples are difficult to procure due to the material compressibility. Moreover, use of the equipment requires some expertise. Microphones must be phase calibrated, and the impedance tube must be well sealed. If the complex wavenumber and characteristic impedance are desired, the two-load method (i.e., ASTM E2611) is generally applied. However, the measurements and data processing are even more complicated (Hua et al., 2015).

There is a less complicated approach to determine the sound absorption coefficient. The flow resistivity is first measured using ASTM C522 (2009). This measurement is more forgiving than impedance tube measurements and may be executed by entry-level engineers. The necessary equipment can be constructed using off-the-shelf pipes and less sophisticated measurement equipment. A data acquisition system is not required. Once the flow resistivity of the material is

measured, the data can be input into empirical equations. Delany and Bazley (1970) and Mechel (1988) developed empirical equations for fibers, and Wu (1988) developed similar expressions for plastic foams.

For many engineering purposes, determining the sound absorptive properties via measurement of flow resistivity is sufficient. However, sound absorbing materials have been developed in the intervening years since the empirical equations were developed. Wu measured foams having flow resistivities between roughly 2900 and 25,000 rayls whereas modern-day commercially available foams sometimes have flow resistivities exceeding 25,000 rayls. Moreover, it is unclear whether the empirical equations are truly representative of the range of fiber and foam products available today.

The objective of this work was to provide flow resistivity information for a number of sample absorbers that were provided to the University of Kentucky. This data can be used to determine the normal incidence impedance or bulk properties, which can then be inserted into simulation models. The table should be useful to analysts in the early design stages who are seeking inputs to their models.

Rather than relying on the measured flow resistivity to determine the sound absorptive properties, the sound absorption coefficient was measured using ASTM E1050 (2012) and the flow resistivity determined by minimizing the least squared error between the measured and calculated sound absorption. Different processing schemes for performing the curve fit are discussed and compared.

3.1.1 Materials Selection

Ten different samples were procured from vendors for the initial materials database. They include 3 glass fibers and 7 foams. The materials selected are representative of those commonly used in industrial applications.

1. Miscellaneous Foam
2. Melamine Foam
3. Polyether Foam
4. Polyester Fiber
5. Polyester Fiber
6. Polyester Foam
7. Polyimide Foam
8. Polyester Foam
9. Glass Fiber
10. Polyurethane Foam

Figure 3.1 Ten different samples for database

3.2 Least Squares Data Fitting

The sound absorption was measured in an impedance tube according to ASTM E1050 and then a least squares curve fit was used to identify the flow resistivity which would result in the smallest error. The approach used by Simón et al. (2006) is adopted here but some improvements are made. Two different approaches were considered for error minimization. In the first, the error in sound absorption

.

was minimized using a linear scale. In that case, the objective is to minimize the function

$$F(\sigma) = \sum_{i=1}^{N} \left(\alpha_i(\sigma) - \alpha_{i,meas}\right)^2 \tag{3.1}$$

where $\alpha_i(\sigma)$ and $\alpha_{i,meas}$ are the sound absorptions determined from the empirical equations and measurement respectively. The objective of the optimization is to determine the flow resistivity that will minimize the error.

Since sound pressure is normally reported on a logarithmic scale for most industrial applications, Ebbitt et al. (2013) and others have suggested that the sound absorption should be plotted on a logarithmic scale as well. Minimizing the least squares error can take on a similar form. In that case, the objective is to minimize the error after taking the logarithm of the sound absorption. This is expressed as

$$\min_{(\sigma)} \sum_{i=1}^{N} \left(\log(\alpha_i(\sigma)) - \log\left(\alpha_{i,meas}\right)_i\right)^2 \tag{3.2}$$

It seems reasonable to prefer Equation 3.2 to Equation 3.1.

In Equations 3.1 and 3.2, i is an index for different frequencies being considered. Simón et al. (2006) selected evenly spaced frequencies. However, sampling at evenly spaced frequencies will skew the curve fit towards the higher frequencies. In this paper, 1/12th octave band center frequencies are selected for the error minimization so that equal weighting is given to each octave band when

.

determining the least squares error. The 1/12th octave band sampling is illustrated in Figure 3.2.

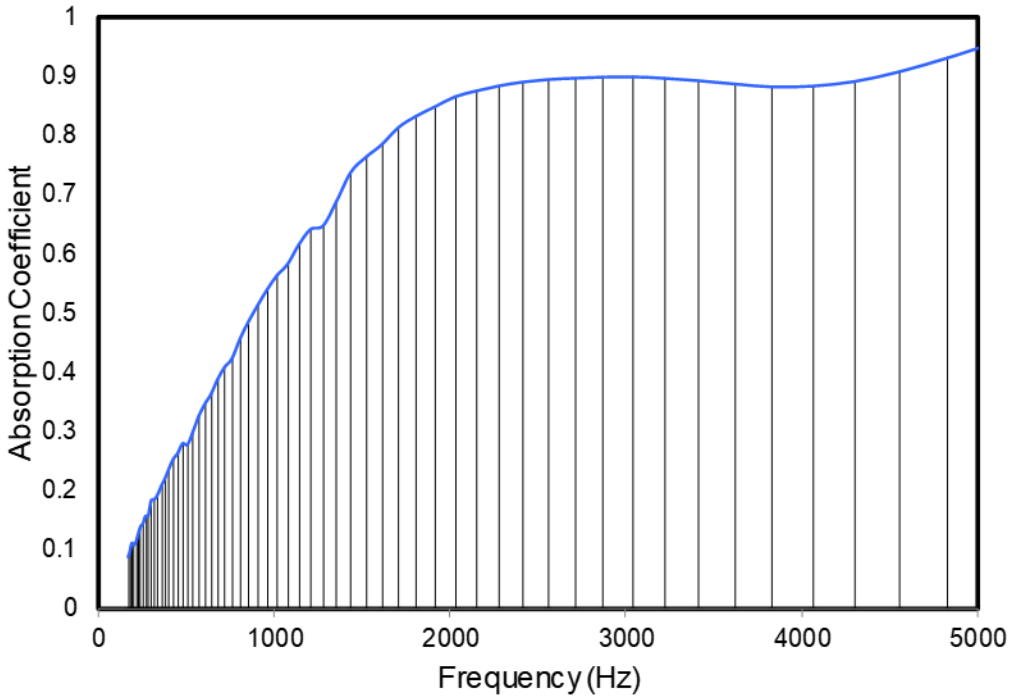

Figure 3.2 Plot illustrating sampling at the 1/12th octave band center frequencies.

3.3 Microstructure of Fibers and Foams

Sound absorbing materials convert acoustic energy to heat or vibration. Hence, the microstructure of the sound absorbing material governs the sound absorbing potential. Photos of ten different materials under microscope are taken and the photos are post processed by *Image J* (Rasband, NIH), and the porosity and average pore size of the foam and the fiber size of fibrous material were determined. Figures 3.3 shows the microstructure of the melamine foam and polyester fiber respectively.

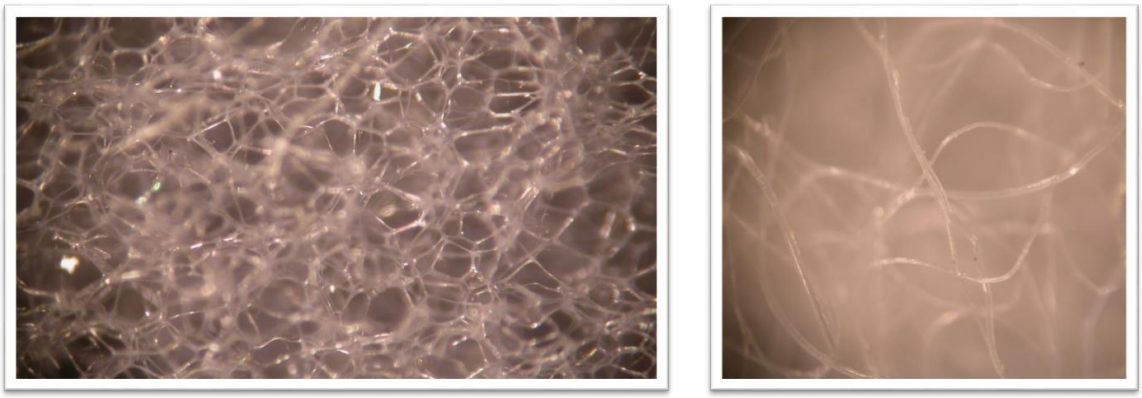

a) b)

Figure 3.3 a) Microstructure of melamine foam. b) Microstructure of polyester fiber.

The porosity and average porous size of the foam and the fiber size of fibrous material are measured by the software and listed in Table 3.1:

Table 3.1 Microstructure properties of porous materials

Name	Type	Fiber Size (um)	Porous size (um^2)	Porosity (%)
Polyester Fiber	Fibrous	34		
Polyester Fiber	Fibrous	49		
Glassfiber	Fibrous	9		
Polyimide	Fibrous	50		
Polyether	Foam		423	77
Misc. Foam	Foam		421	76
Polyester	Foam		418	68
Polyester	Foam		279	59
Melamine	Foam		46	73
Polyurethane	Foam		289	64

The melamine sample has the smallest porous size and a high porosity can be observed from the table. This kind of pore structure make melamine an outstanding

sound absorbing material. This table can be used to analyze the relationship between the microstructure of the sound absorbing materials and its absorption.

3.4 Flow Resistivity for Fibers and Foams

In the discussion that follows, *Method A* uses Equation 3.1 with a frequency spacing of 10 Hz for the curve fit. *Method B* uses Equation 3.2 with the even 10 Hz frequency spacing. *Method C* uses Equation 3.2 but samples the data at the 1/12th octave band frequencies. Figure 3.4 compares the sound absorption coefficient for 20 mm fiber. Notice that *Methods A*, *B*, and *C* are in good agreement with one another. Data is only shown above 300 Hz because the measured results are noisy below that frequency. Figure 3.5 shows a similar comparison for 28.5 mm thick polyurethane foam. Notice that the curve fits agree well with the measured data.

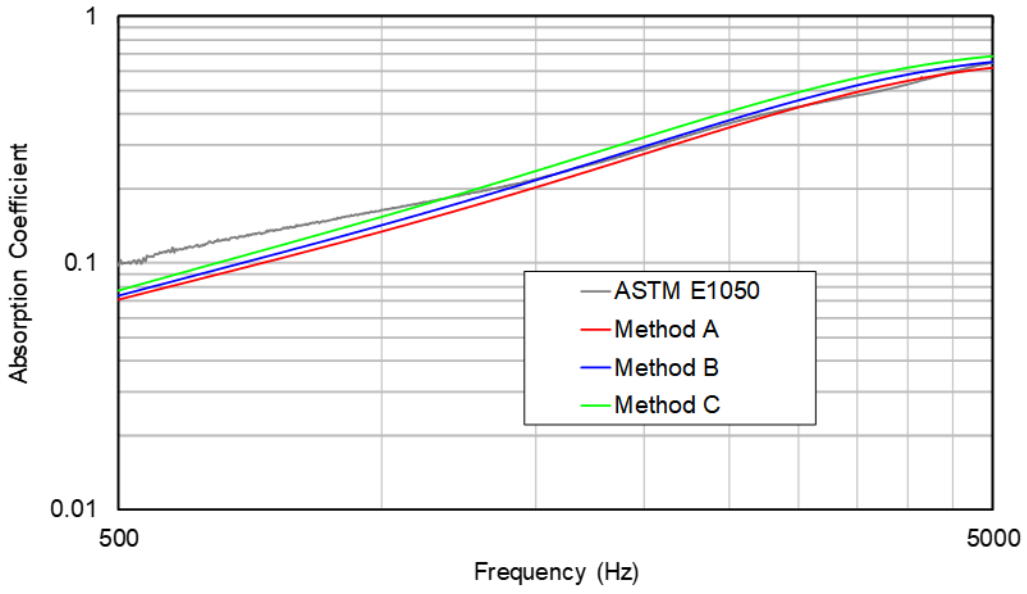

Figure 3.4 Sound absorption coefficient for 20 mm thick polyester fiber.

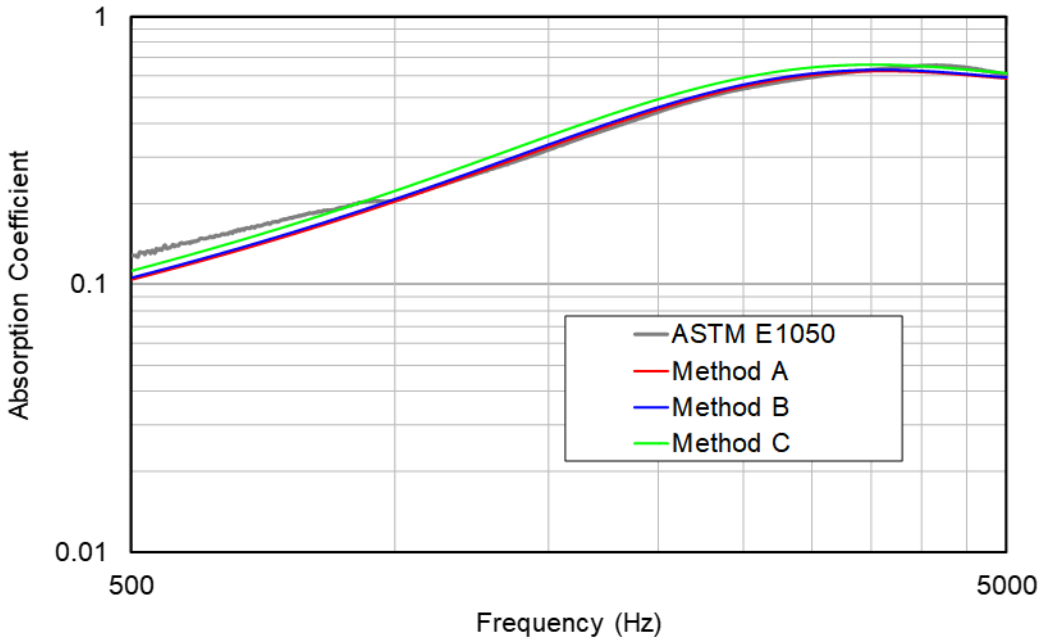

Figure 3.5 Sound absorption coefficient for 28.5 mm thick polyurethane foam.

Figures 3.6 and 3.7 compare the predicted complex characteristic impedance and complex wavenumber respectively obtained via *Method C* for 20 mm fiber. Results agree well with direct measurement using the two-cavity approach (Utsuno et al., 1989). Similar results were also obtained for 24 mm melamine foams and are shown in Figures 3.8 and 3.9.

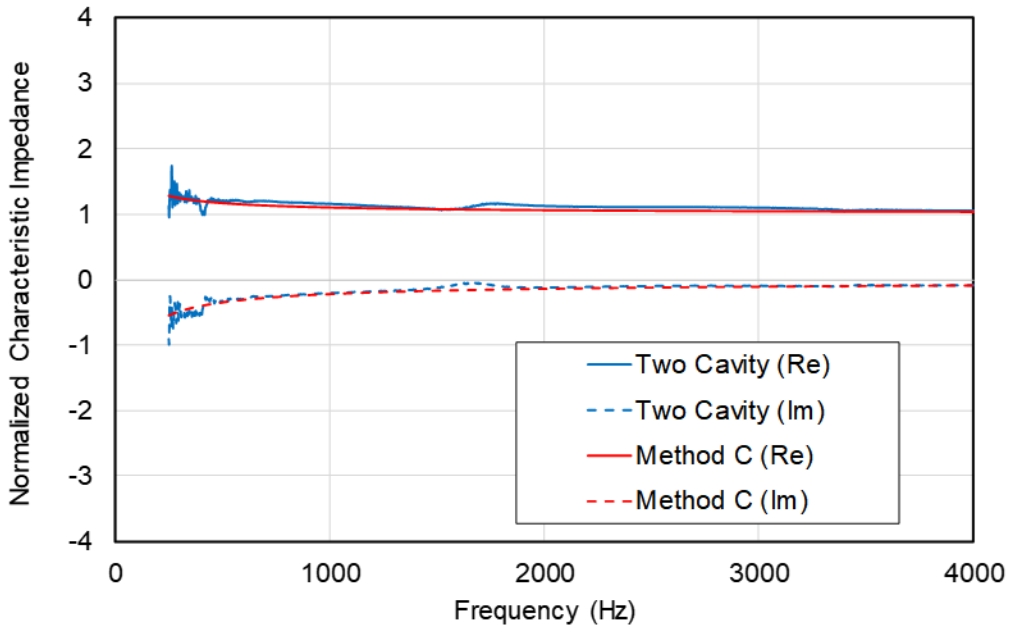

Figure 3.6 Normalized characteristic impedance for a 20 mm thick polyester fiber.

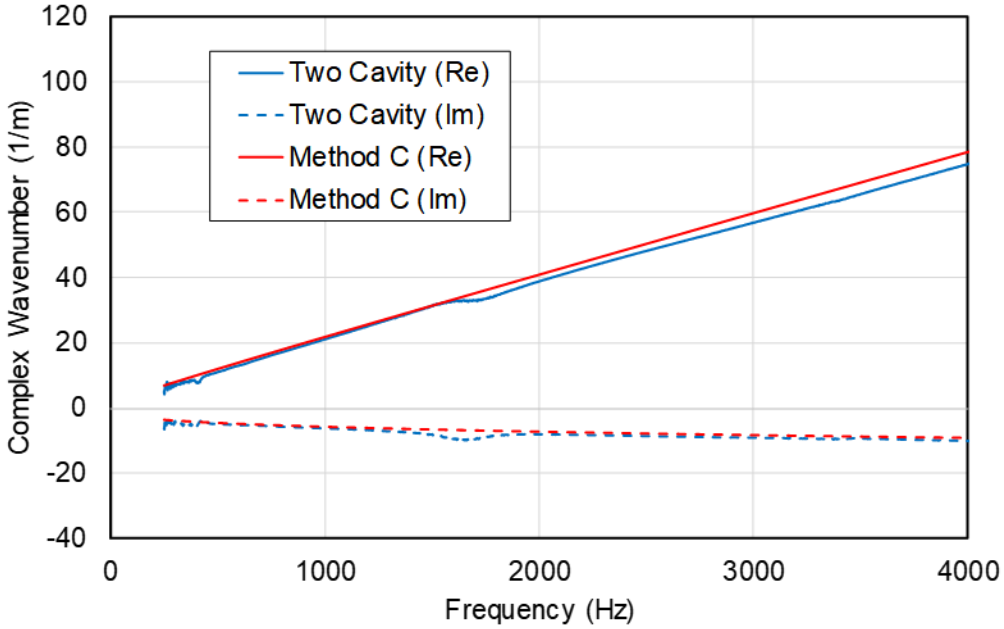

Figure 3.7 Complex wavenumber for a 20 mm thick polyester fiber.

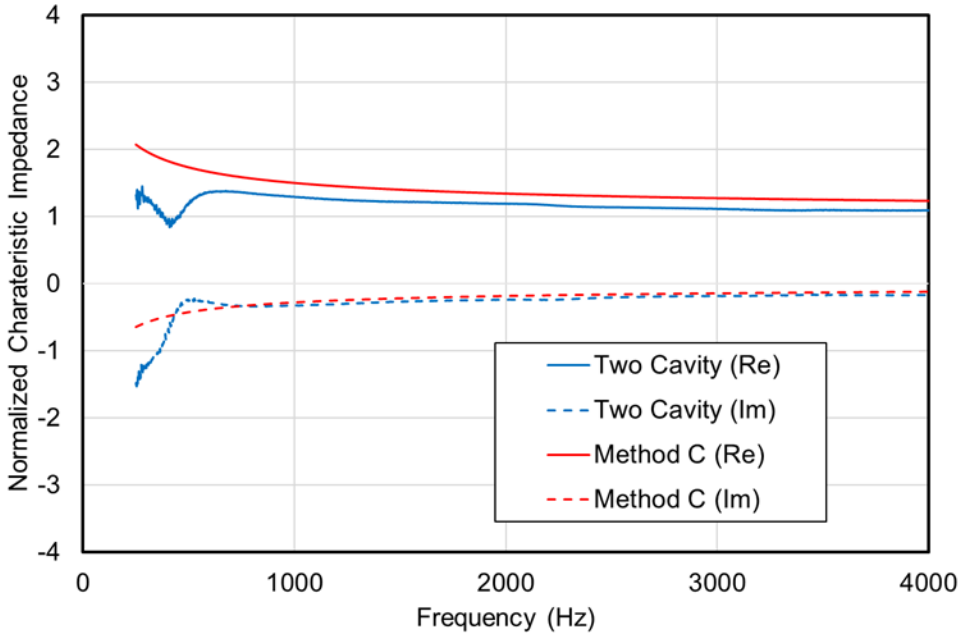

Figure 3.8 Normalized characteristic impedance for a 24 mm thick melamine foam.

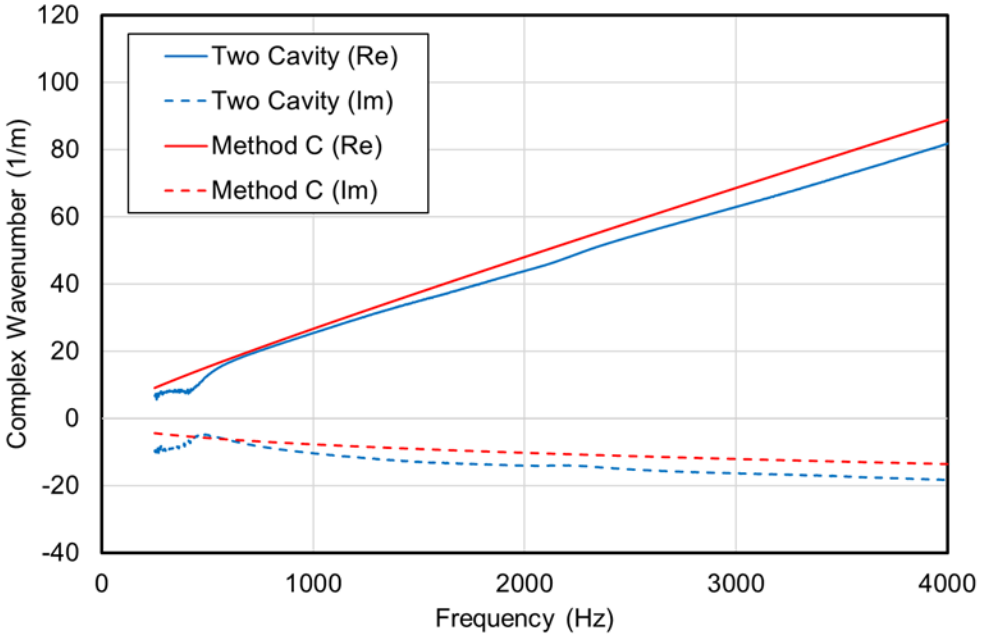

Figure 3.9 Complex wavenumber for a 24 mm thick melamine foam.

The flow resistivity was obtained using *Methods A, B,* and *C* for 3 fiber samples and 7 foam samples. Mechel's (1988) and Wu's (1988) material models were used for fiber and foam samples respectively. The flow resistivity was also measured directly using ASTM C522 (2009). Notice that *Methods A*, *B*, and *C* generally agree well with each other and direct measurement of flow resistivity. Differences will only minimally affect the calculated sound absorption.

Table 3.2 Flow resistivities determined for several different commercial fibers and foams.

Name	Density (kg/m^3)	Method A (rayls/m)	Method B (rayls/m)	Method C (rayls/m)	Direct Method (rayls/m)
Polyester Fiber	27	2380	2460	2800	2400
Polyester Fiber	44	1280	1330	1610	1260
Glass Fiber	124	48800	50700	62700	54000
Melamine Foam	9	7460	7710	7970	8400
Polyurethane Foam	19	2150	2190	2560	1930
Polyether Foam	16	10450	9600	8770	9930
Misc. Foam	29	4380	4350	4960	4960
Polyester Foam	29	15250	14060	13000	12590
Polyester Foam	24	4210	4060	4410	4310
Polyimide	7	9740	11160	19100	256000

3.5 Application to Layered Materials

The curve fitted flow resistivity results from the previous section were utilized to determine the sound absorption for two double layer sound absorbers. Including *Sample 1*: 20 mm thick polyester fiber and 28.5 mm thick polyurethane foam and

Sample 2: 26 mm polyether foam and 24 mm melamine foam. The sound absorption for the double layer samples were measured and then predicted from the flow resistivities using *Method C*. The double layer samples were then measured using ASTM E1050 (2012). Figures 3.10 and 3.11 compare the measured and predicted sound absorption coefficients for samples *1* and *2* respectively. It can be observed that there is good agreement between the predictions and measurement.

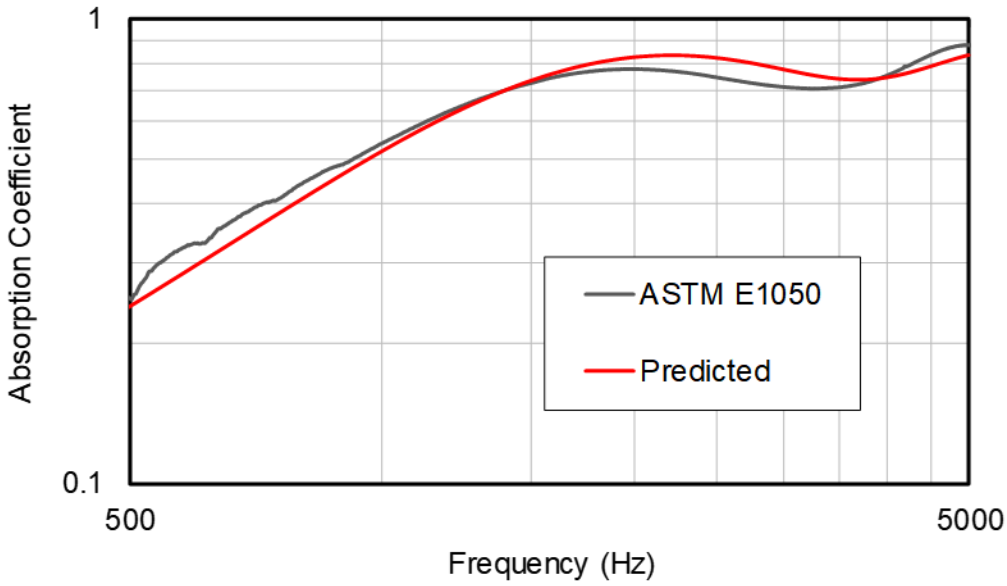

Figure 3.10 Sound absorption comparison for a 20 mm polyester fiber and 28.5 mm polyurethane foam.

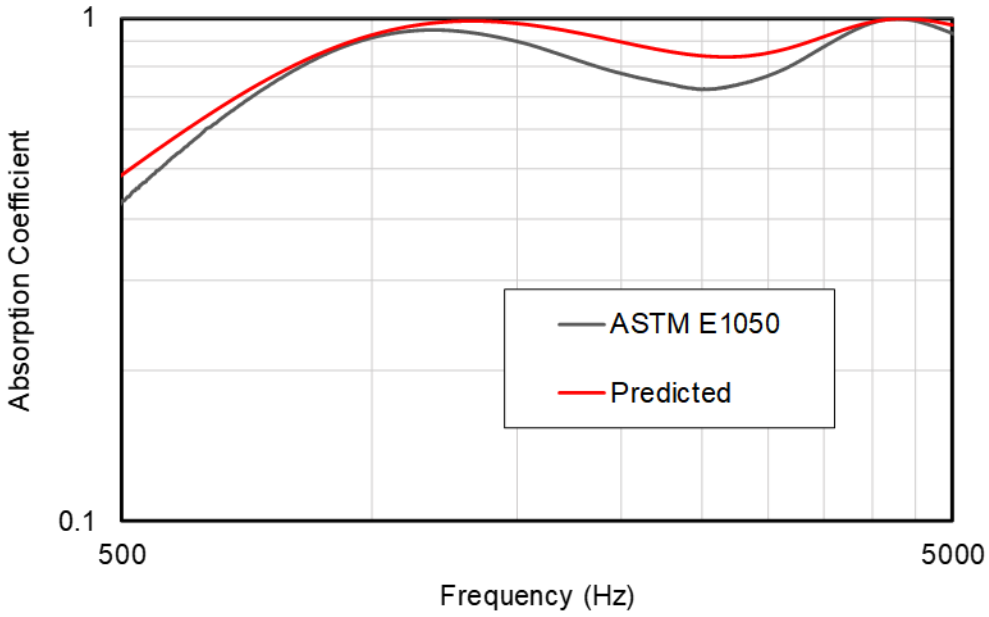

Figure 3.11 Sound absorption comparison for a 26 mm polyether foam and 24 mm melamine foam.

3.6 Conclusions

The flow resistivity of a number of commercial sound absorbing materials was characterized using an indirect measurement approach. The sound absorption coefficient was measured in an impedance tube and was compared against empirical equations that depend on the flow resistivity. The value for the flow resistivity was optimized to produce a best match between the measurement and empirical equations. It was recommended to minimize the least square error for the sound absorption on a logarithmic scale rather than a linear scale and to sample the data at the 1/12th octave band center frequencies. Flow resistivities from the resulting database were then used to predict the sound absorption for layered materials.

Chapter 4 Bulk Properties of Compressed Materials

Sound absorbing materials are commonly compressed when installed in passenger compartments or underhood applications altering the sound absorption performance of the material. However, most prior work has focused on uncompressed materials and only a few models based on poroelastic properties are available for compressed materials. Empirical models based on flow resistivity are commonly used to characterize the complex wavenumber and characteristic impedance of uncompressed sound absorbing materials from which the sound absorption can be determined. In this chapter, the sound absorption is measured for both uncompressed and compressed samples of fiber and foam, and the flow resistivity is curve fit using an appropriate empirical model. Following this, the flow resistivity of the material is determined as a function of the compression ratio.

4.1 Introduction

Sound absorbing materials are frequently compressed during installation. Though it is well known that installation will greatly impact the sound absorptive properties, surprisingly little work has been performed on this topic. The primary work has been that of Castagneáde et al. (2000) who looked at the effect of compression on the input parameters to the Johnson-Allard (Johnson,1987, Allard,1993) model. The input parameters include tortuosity, flow resistivity, thermal characteristic length, and porosity. The study was limited to fibrous materials and it was assumed that the properties of the uncompressed media had been previously measured.

.

Several similar studies have built on the efforts of Castagneáde et al. (2000). Wang et al. (2008) improved on the model by including the stiffness of the elastic frame. Ohadi and Moghaddami (2007) integrated the relationships developed by Castagneáde et al. (2000) into finite element simulations of compressed porous materials. Kino et al. (2009) examined compressed melamine, and Geslain et al. (2001) narrowed their focus to determining the compressed elastic modulus of the elastic frame. Each of the aforementioned studies assumed the Johnson-Champoux-Allard model as a starting point.

In this chapter, the flow resistivity of compressed sound absorbers is determined by measuring the absorption and then curve fitting to the empirical models already detailed in Section 2.4. The primary advantage of this method is simplicity. No special equipment, aside from an impedance tube, is required since tortuosity, porosity, and viscous characteristic length is not measured.

4.2 Measurement Approach

The approach utilized for determining the flow resistivity of the sample follows that of Simón et al. (2006) and is summarized in Figure 4.1. The sound absorption (α) is first measured using ASTM E1050 (2012). Following this, guesses for the flow resistivity are inserted into an appropriate empirical equation until the least squares error is minimized between the predicted and measured sound absorption. Since the empirical equations are based on flow resistivity, materials which are governed by structural damping instead of viscous losses (i.e., closed cell foams) are not amenable to this approach.

.

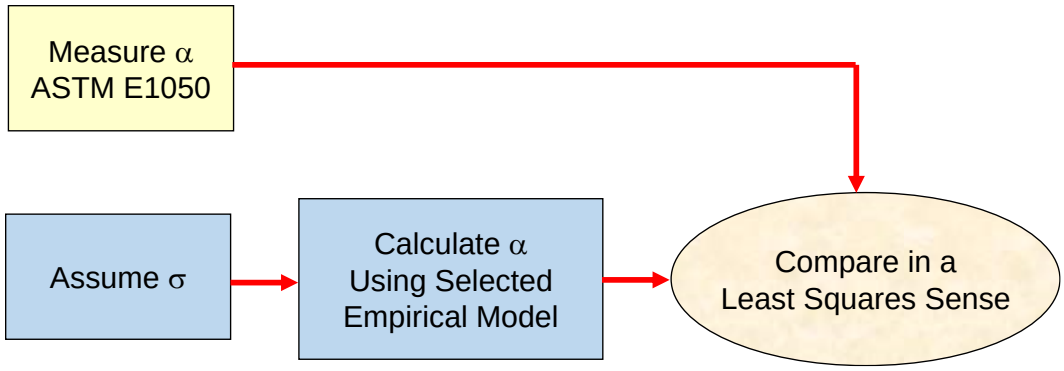

Figure 4.1 Least square error minimization approach to determine the sound absorption

The sample is compressed using the wire cloth shown in Figure 4.2. The wire cloth is positioned on the side of the sample facing the loudspeaker and covers the sample compressing it against the rigid end of the impedance tube. It is assumed that the sample compresses uniformly. This is likely the case for lightly compressed fibers, but it is probably not the case for foams.

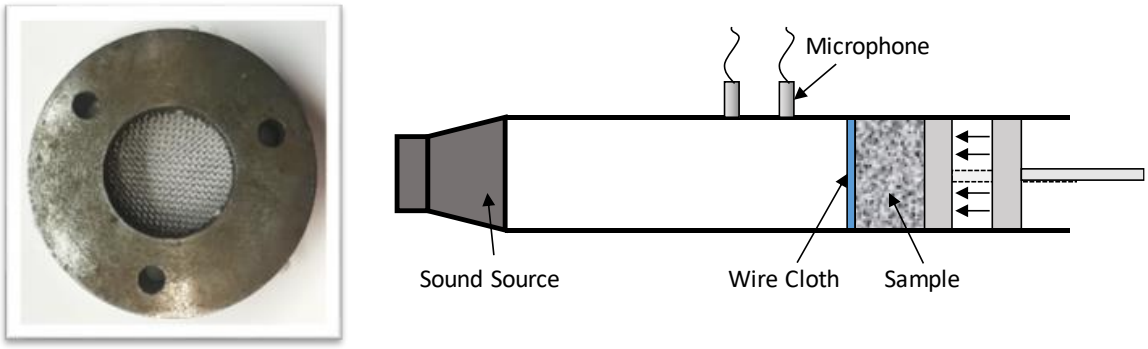

a) b)

Figure 4.2 a) Photograph of wire cloth. b) Schematic showing positioning of sample and wire cloth in the impedance tube.

The complex wavenumber and characteristic impedance of selected samples were also measured to ensure that the predicted properties compared well with those

measured. The three-microphone method was used to measure the bulk properties. The method was originally developed by Salissou and Panneton (2010) and is detailed in Section 2.3.3.

4.3 Measurement Validation

To ensure that the wire cloth has a minimal effect on the sound absorption measurement, a sample was measured with and without the wire cloth. Figure 4.3 shows the comparison from which it is evident that the wire cloth has a minimal impact on the sound absorption.

It was also confirmed that the empirical equations could be fitted to the measured compressed sound absorption. Figures 4.4 and 4.5 show the measured compressed sound absorption compared with the fitted data for 40 mm thick polyester fiber and 24 mm thick melamine foam respectively. For the fiber, the curve fit compares well with the measurement. However, there are some discrepancies for the melamine foam since the compression leads to additional structural modes in the elastic frame. Nonetheless, the empirical model provides a reasonable fit on average.

.

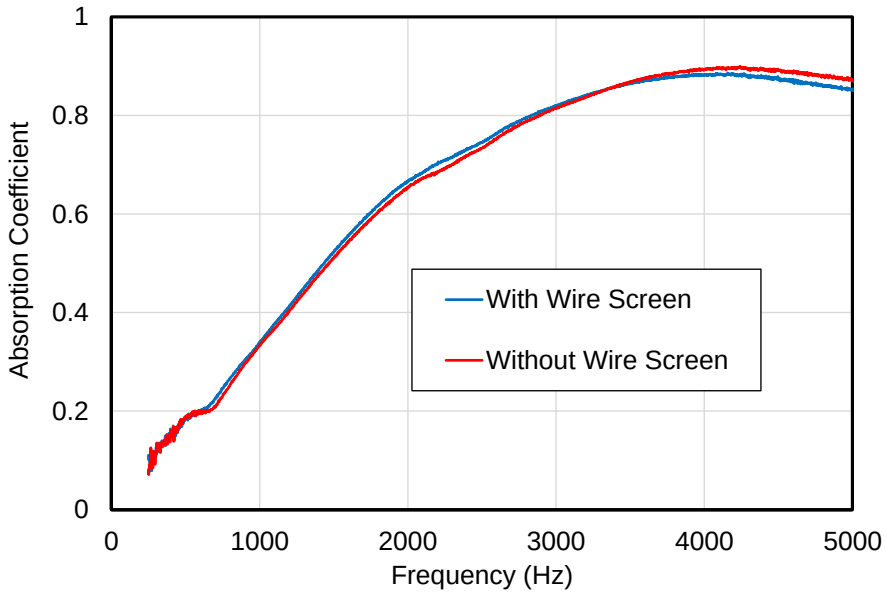

Figure 4.3 Comparison of sound absorption for 24 mm thick melamine with and without the wire screen.

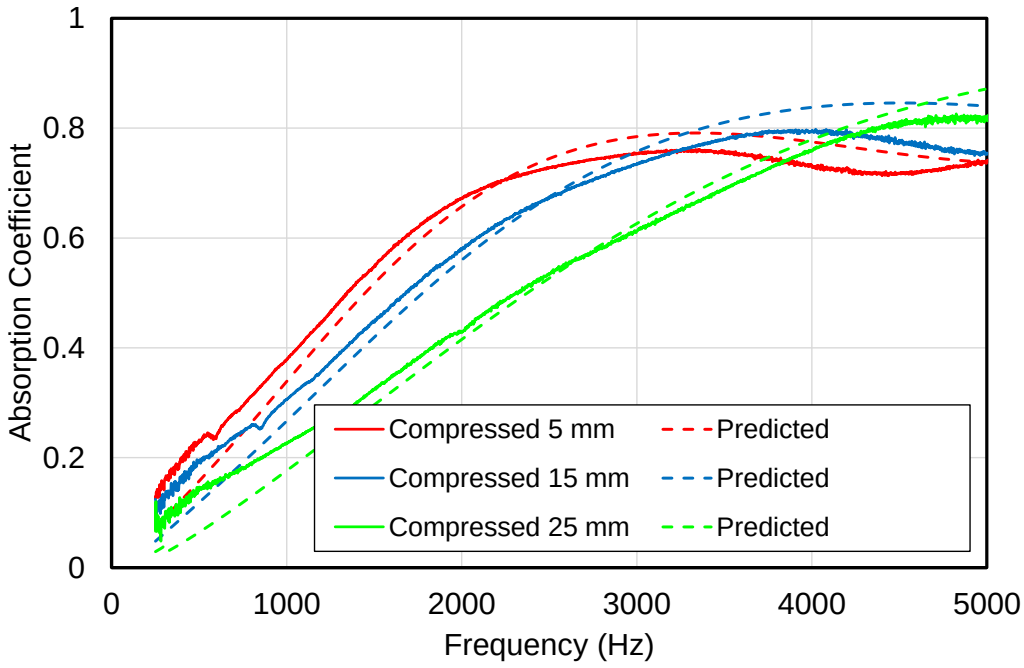

Figure 4.4 Comparison of predicted and measured sound absorption for 40 mm thick polyester fiber under different compression.

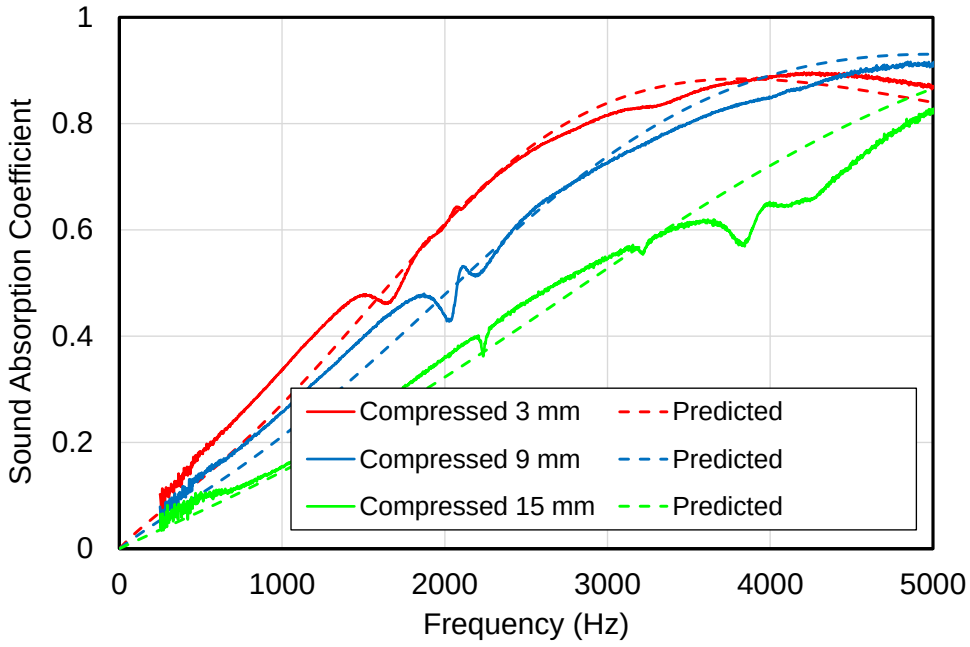

Figure 4.5 Comparison of predicted and measured sound absorption for 24 mm thick melamine foam under different compression.

The bulk properties were also checked for the 40 mm thick polyester fiber. The complex wavenumber and characteristic impedance are compared in Figures 4.6 and 4.7 respectively. Results are shown for the uncompressed material and for the material compressed 16 mm. This corresponds to a compression ratio of 1.67. Though only the sound absorption is fitted, the more fundamental bulk reacting properties also compare well with one another. Figures 4.8 and 4.9 show similar results for 24 mm thick melamine foam. As before, the fitted curve trends well with the measured result. These results demonstrate that a fit based on sound absorption can be used to determine the more fundamental bulk properties (i.e. complex wavenumber and characteristic impedance). This assumption should be confirmed on other materials as well.

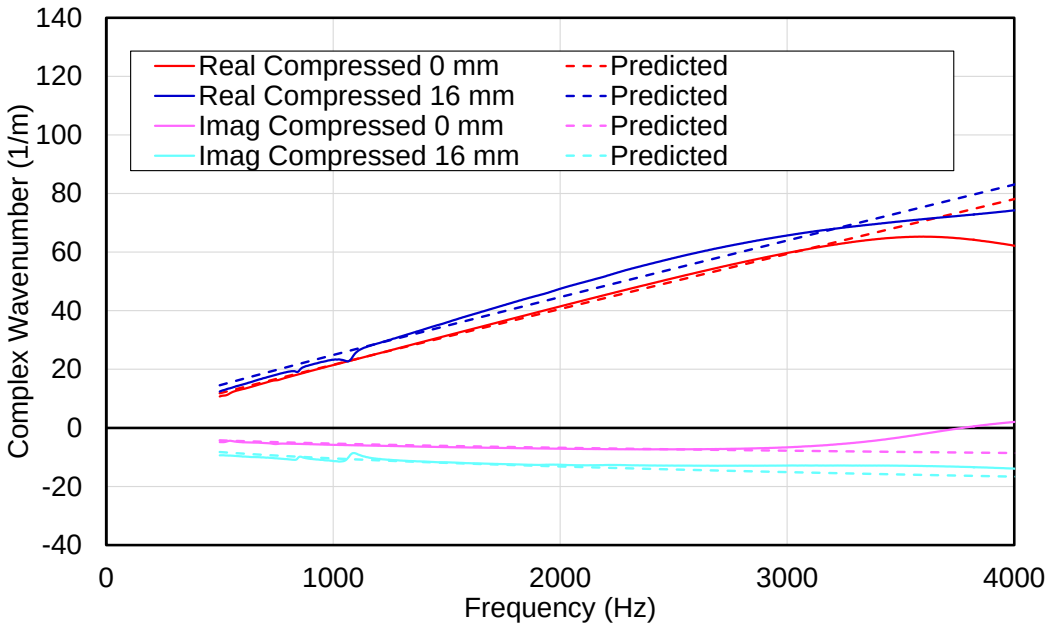

Figure 4.6 Comparison of predicted and measured real and imaginary parts of the complex wavenumber for 40 mm thick polyester fiber.

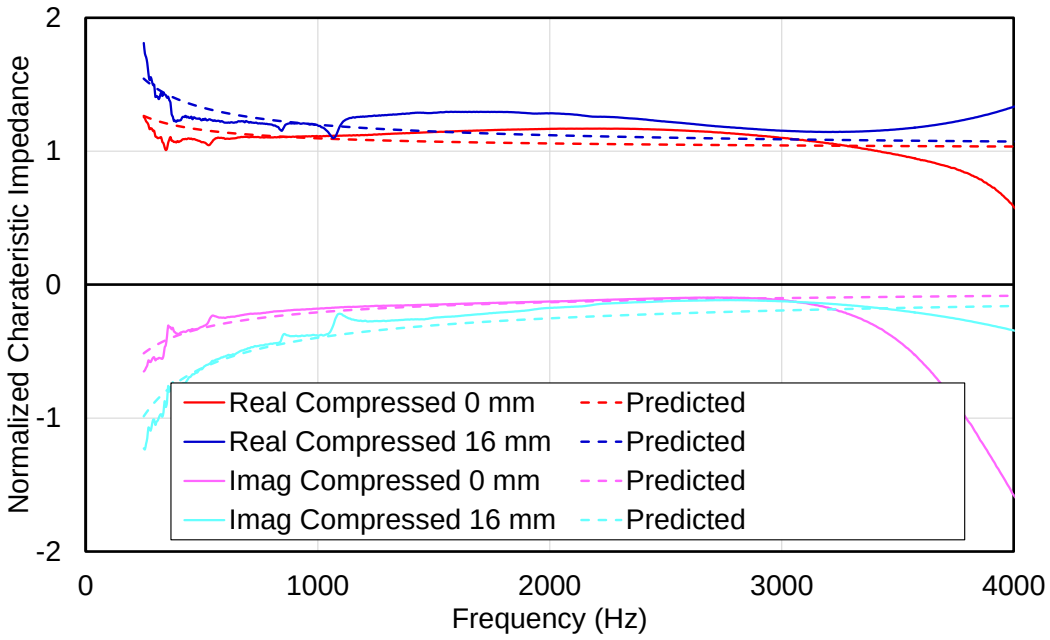

Figure 4.7 Comparison of predicted and measured real and imaginary parts of the characteristic impedance for 40 mm thick polyester fiber.

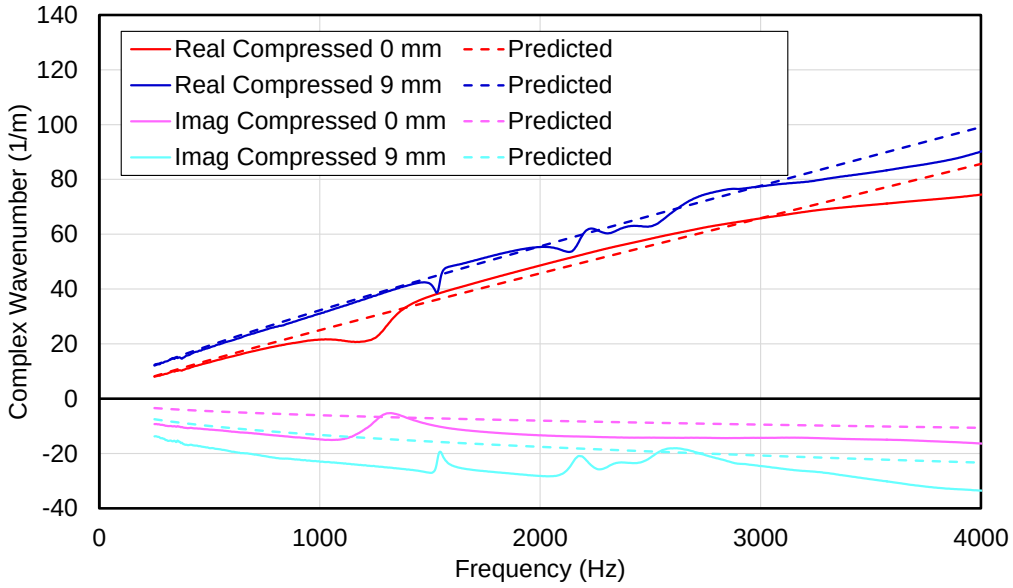

Figure 4.8 Comparison of predicted and measured real and imaginary parts of the complex wavenumber for 24 mm thick melamine foam.

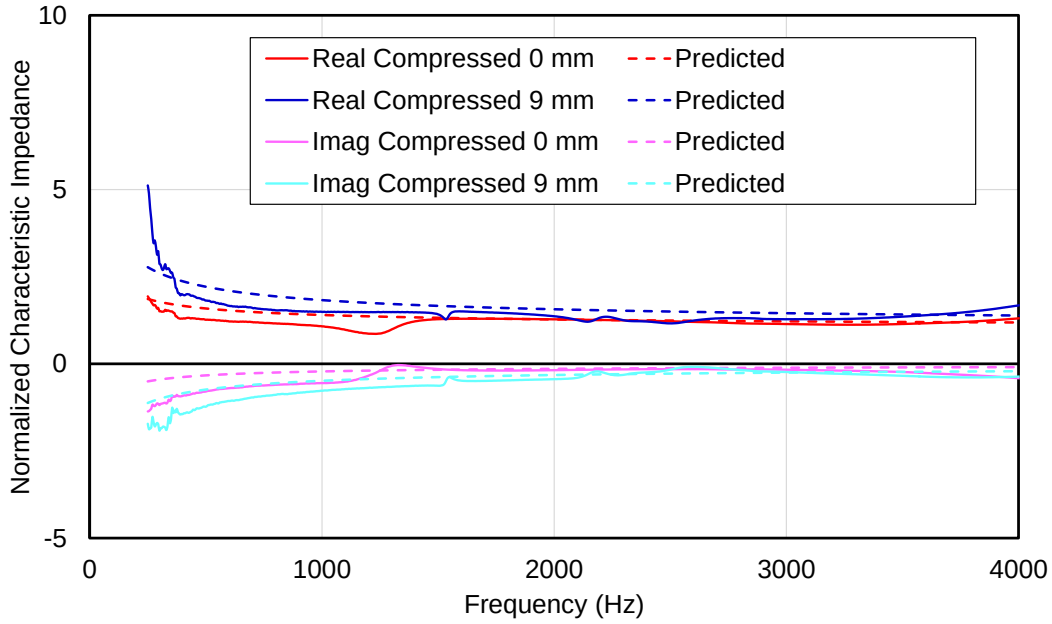

Figure 4.9 Comparison of predicted and measured real and imaginary parts of the normalized characteristic impedance for 24 mm thick melamine foam.

4.4 Results

Compression studies were performed on two fibers (glass wool and polyester) and melamine foam. Each sample was compressed in 1 mm increments and the sound absorption was measured at each increment. Following this, the flow resistivity at each increment was determined using the least squares curve fitting procedure laid out earlier in the paper. The fibers were fitted using Mechel (1988) whereas the foams using Wu (1988).

Castagneáde et al. (2000) used a simple equation relating the flow resistivity to the compression ratio (n_c), which is defined as the ratio of the original to the compressed thickness. One-dimensional compression is assumed and the flow resistivity of the compressed sample can be expressed as

$$\sigma = n_c \sigma_o \tag{4.1}$$

where σ_o is the uncompressed flow resistivity. Alternatively, Castagneáde et al. (2000) suggested that the modified flow resistivity is proportional to the compression ratio squared (n_c^2) for the case of two-dimensional compression. This may be more appropriate for the case of foams. Wang et al. (2008) and Ohadi and Moghaddami (2007) assumed one-dimensional compression. Kino et al. (2009) used different assumptions depending on the material. In this work, a linear curve fit is used. Though a quadratic fit can be argued for, a linear fit seems to be sufficient for engineering applications.

The flow resistivity is plotted versus the compression ratio for glass wool, polyester fiber, and melamine foam in Figures 4.10, 4.11, and 4.12 respectively. The linear

curve fit is also indicated on the plots as well. Table 4.1 shows the linear equations for each material.

Table 4.1 Equations for the flow resistivity as a function of compression ratio.

Material	Equation
Glass Wool	$\sigma = 13500n_c - 6470$
Polyester Fiber	$\sigma = 6990n_c - 5080$
Melamine Foam	$\sigma = 25300n_c - 20900$

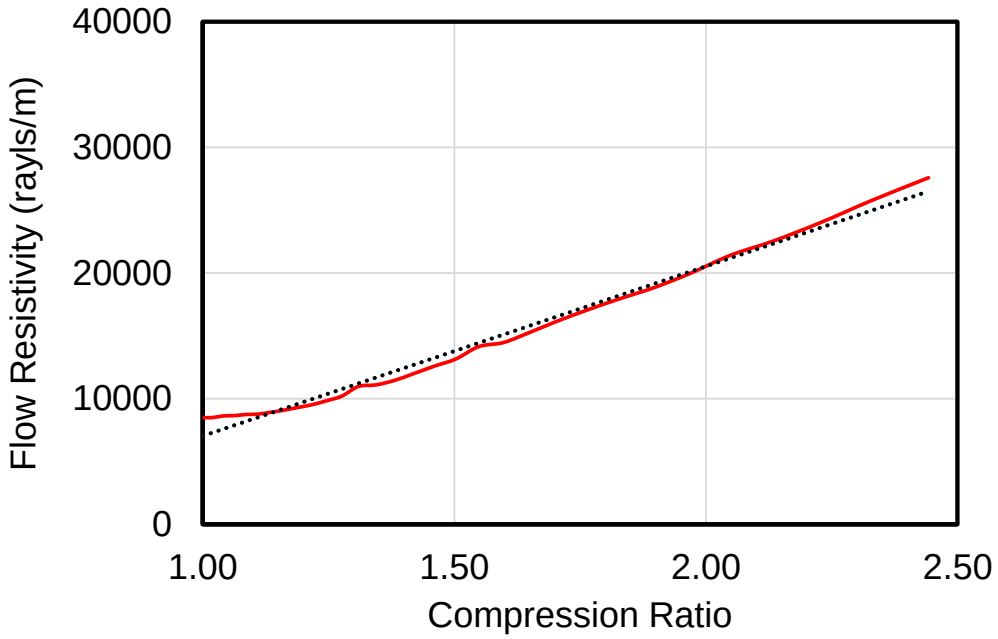

Figure 4.10 Plot of the flow resistivity versus the compression ratio for 50.8 mm glass wool. The linear curve fit is indicated by the dashed line.

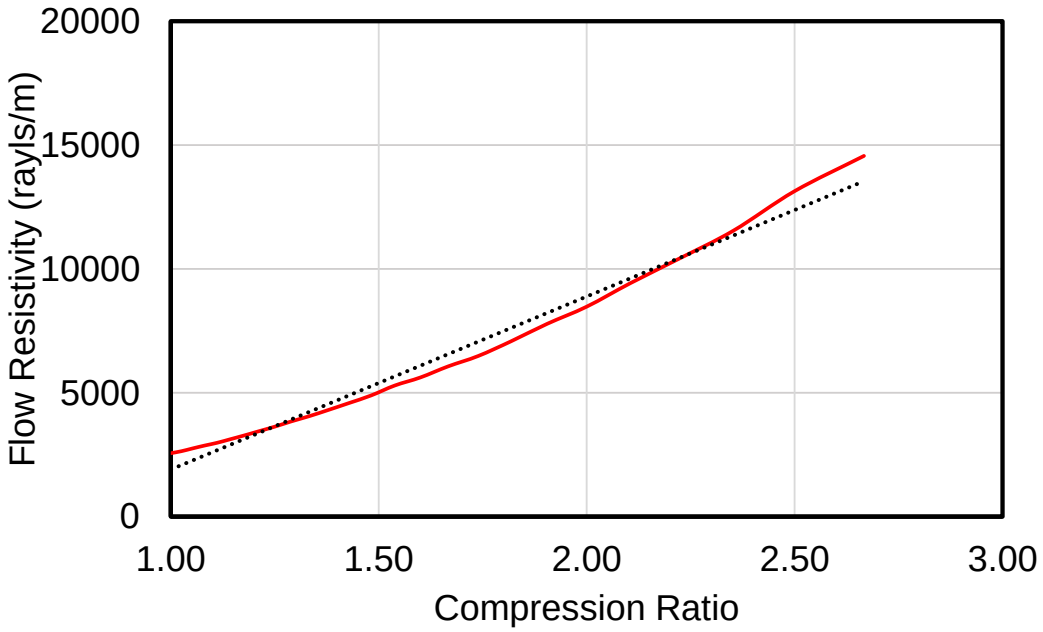

Figure 4.11 Plot of the flow resistivity versus the compression ratio for 40 mm polyester fiber. The linear curve fit is indicated by the dashed line.

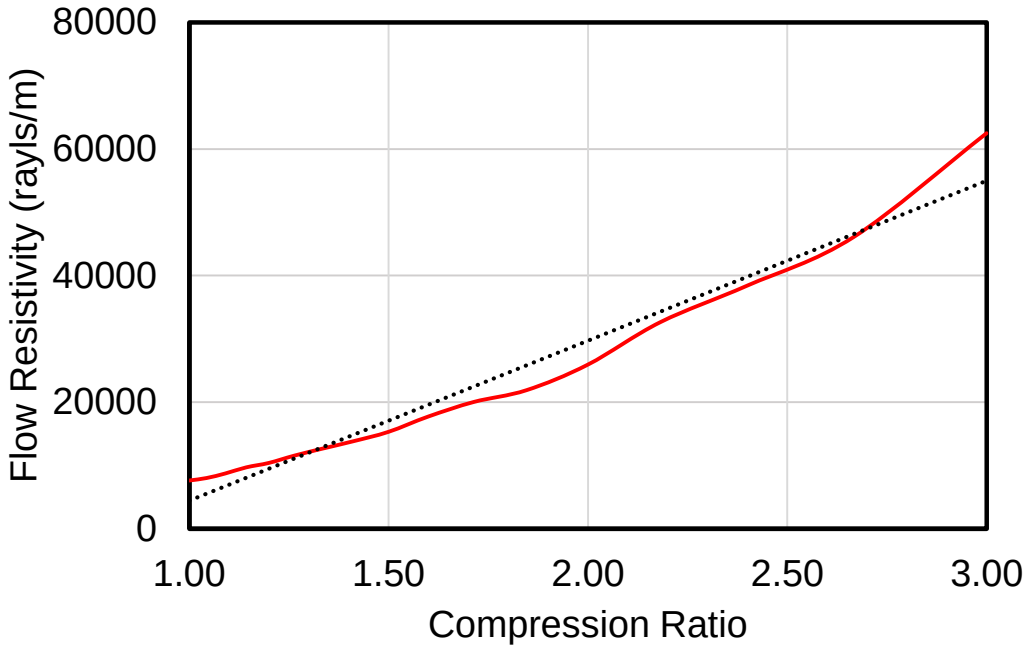

Figure 4.12 Plot of the flow resistivity versus the compression ratio for 24 mm melamine foam. The linear curve fit is indicated by the dashed line.

4.5 Conclusions

An approach has been suggested for characterization of compressed materials. The sound absorption of the compressed sample is measured. A flow resistivity is then selected that produces the best fit prediction to the measured sound absorption. The approach was applied and worked well for both fiber and foam samples. It was shown that linear equations could be developed that relate the flow resistivity to the compression ratio.

The approach developed is advantageous because it only requires an impedance tube. However, the properties of materials that are compressed during production may be different. The developed approach can be easily applied in industry. Future work will examine the use of the approach to determine the sound absorption of compressed layered materials.

.

Chapter 5 Conclusion and Future Work

5.1 Summary

The main objectives of the research documented in this thesis were to 1) develop a rudimentary materials database based on directly and indirectly measured flow resistivities and 2) develop a simple procedure for determining the sound absorption of compressed materials. In both studies, the flow resistivities for the various sound absorbers were determined using an indirect method. The sound absorption was first measured in an impedance tube according to the two-microphone method standardized in ASTM E1050 (2012) and then curve fit using various material dependent empirical models to determine the flow resistivity. The frequency domain was sampled in various ways to insure the best fit. First, it was sampled in narrow (10 Hz increments) and 1/12 octave bands. Then, the curve fit was also performed on both a linear and logarithmic scale. It is recommended that a logarithmic scale with $1/12^{th}$ octave frequencies be used. After settling on a procedure, the flow resistivity of 10 common sound absorptive materials was measured and a rudimentary sound absorptive materials database was developed.

The second part of this research was more extensive and looked at the effect of compression on fibers and foams. The flow resistivity was measured for compressed materials in the same manner as before. Samples (two fiber and two foam absorbers) were compressed and the sound absorption was measured. From which, the flow resistivity was determined via curve fit. From the measurements, a relationship between flow resistivity and the compression ratio

was established. This relationship can then be used to predict the sound absorption of compressed layered materials.

The primary contributions of this work are as follows. It was demonstrated that:

1. The choice of empirical model for sound absorption does not have a major impact especially if the curve fitting procedure is used.
2. Some improvement is noted in the lower frequency curve fit if the data is sampled in 1/12th octave bands and if a log scale is used for determining the squared error to be minimized.
3. A wire mesh can be used for compressing materials and it was demonstrated that the wire mesh will not affect the sound absorption measurement.
4. The three-microphone method is especially helpful for determining the bulk properties for compressed materials.
5. Equations relating the flow resistivity to the compression ratio can be developed. Equations of this type can be especially helpful for assessing the properties of compressed layered materials.
6. The flow resistivity approaches discussed in this thesis are sufficient for most engineering applications though perhaps not as accurate as approaches which use phenomenological equations.

5.2 Recommendation

It is recommended that the following studies be performed. Future work should include:

1. Performing similar tests on a number of other sound absorbing materials to increase the number of samples in the database.
2. Comparing similar samples from different manufacturers to gage how different manufacturing processes affect the properties of sound absorbers when uncompressed and compressed.
3. Include the effects of glue and mass layers in compressed sound absorptive materials to prove that such complicated material lay-ups can be simulated using transfer matrix approaches.

REFERENCES

J. Allard and N. Atalla, (2009). *Propagation of Sound in Porous Media: Modelling Sound Absorbing Materials* 2e. John Wiley & Sons.

J. F. Allard and Y. Champoux, (1988). “New empirical equations for sound propagation in rigid frame fibrous materials,” Journal of the Acoustical Society of America **91**, 1002-1013.

ASTM standard, (2010). “Standard Test Method for Measurement of Normal Incidence Sound Transmission of Acoustical Materials Based on the Transfer Matrix Method,” E2611-10.

ASTM standard, (2009). “Standard Test Method for Airflow Resistance of Acoustical Materials,” C522-09.

ASTM standard, (2012). “Standard Test Method for Impedance and Absorption of Acoustical Material Using a Tube, Two Microphones and Digital Frequency Analysis System,” E1050-12.

Y. Atalla and R. Panneton, (2005). “Inverse Acoustical Characterization of Open Cell Porous Media Using Impedance Tube Measurements,” Canada Acoustics, **33**, 11-24.

D. A. Bies and C. H. Hansen, (1980). “Flow Resistance Information for Acoustical Design,” Applied Acoustics **13**(5): 357-391.

M. A. Biot, (1956). “The Theory of Propagation of Elastic Waves in A Fluid-saturated Porous Solid. I. Low-frequency Range,” J. Acoust. Soc. Am. **28**(2), 168-178.

C. Braccesi and A. Bracciali, (1998). “Least Square Estimation of Main Properties of Sound Absorbing Materials Through Acoustical Measurements,” Applied Acoustics, **54**(1), 59-70.

.

B. Castagnède, A. Aknine, B. Brouard and V. Tarnow, (2000). “Effects of Compression on the Sound Absorption of Fibrous Materials,” Applied Acoustics **61**(2): 173-182.

Y. Champoux, J.F. Allard, (1991) “Dynamic Tortuosity and Bulk Modulus in Air-Saturated Porous Media,” Journal of Applied Physics **70**(4), 1975-1979.

M. E. Delany and W. A. Bazley, (1970). “Acoustical Properties of Fibrous Absorbent Materials,” Applied Acoustics **3**, 105-116.

P. Dunn and W. A. Davern, (1986). “Calculation of Acoustic Impedance of Multi-Layer Absorbers,” Applied Acoustics **19**, 321-334.

G. Ebbitt, T. Remtema and J. Scheick, (2013). “Sound Absorbers in Small Cavities,” *2013 SAE Noise and Vibration Conference*, 2013-01-1945.

L. J. Eriksson, (1980). “Higher Order Mode Effects in Circular Ducts and Expansion Chambers,” The Journal of the Acoustical Society of America, **68**(2), 545-550.

M. Garai and F. Pompoli, (2005). “A Simple Empirical Model of Polyester Fibre Materials for Acoustical Applications,” Applied Acoustics **66**(12), 1383-1398.

A. Geslain, O. Dazel, J. P. Groby, S. Sahraoui, et al., (2011). “Influence of Static Compression on Mechanical parameters of Acoustic Foams,” Journal of the Acoustical Society of America **130**(2): 818-825.

X. Hua, Y. Zhang, and D.W. Herrin, (2015). “The Effect of Conical Adaptors and Choice of Reference Microphone When Using the Two-Load Method for Measuring Muffler Transmission Loss,” Applied Acoustics **93**, 75-87.

T. Iwase, Y. Izumi and R. Kawabata, (1998). “A New Measuring Method for Sound Propagation Constant by Using Sound Tube Without Any Air Spaces Back of a Test Materials,” *Inter-Noise 98*, New Zealand.

D. L. Johnson, J. Koplik, Dashen, (1987). “Theory of Dynamic Permeability and Tortuosity in Fluid-Saturated Porous Media,” Journal of fluid mechanics **176**, 379-402.

.

N. Kino, T. Ueno, Y. Suzuki and H. Makino, (2009). “Investigation of Non-Acoustical Parameters of Compressed Melamine Foam Materials,” Applied Acoustics **70**(4): 595-604.

F. P. Mechel, (1988). “Design Charts for Sound Absorber Layers,” Journal of the Acoustical Society of America **83**, 1002-1013.

Y. MiKi, (1990). “Acoustical Properties of Porous Materials. Modifications of Delany-Bazley models,” Journal of the Acoustical Society of Japan (E) **11.1**, 19-24.

A. R. Ohadi, and M. Moghaddami, (2007). “Investigating the Effects of Fibrous Material Compression on the Acoustical Behavior of Absorption and Barrier Materials,” Journal of Vibration and Acoustics **129**(2): 133-140.

J. Pan and P. Jackson, (2009). “Review of Test Methods for Material Properties of Elastic Porous Materials,” *SAE Int. J. Mater. Manuf.* **2**(1), 570-579.

R. Panneton and X. Olny, (2006). “Acoustical Determination of the Parameters Governing Viscous Dissipation in Porous Media,” J. Acoust. Soc. Am. **119**, 2027-2040.

W. S. Rasband, ImageJ, U. S. National Institutes of Health, Bethesda, Maryland, USA, https://imagej.nih.gov/ij/, 1997-2016.

Y. Salissou and R. Panneton, (2010). “Wideband Characterization of the Complex Wavenumber and Characteristic Impedance of Sound Absorbers,” Journal of Acoustical Society of America, **128**(5), 2868-2876.

F. Simón, D. Fernandez, and J. Pfretzschner, (2006). "A Fitting Method to Estimate the Air Flow Resistivity of Porous Materials," *The 13th International Congress on Sound and Vibration,* Vienna, Austria.

B. H. Song and J. S. Bolton, (2000). “A Transfer-Matrix Approach for Estimating the Characteristic Impedance and Wave Numbers of Limp and Rigid Porous Materials,” Journal of Acoustical of Society of America, **107**(3), 1131–1152.

.

D. R. Stanley, (2012). “Impedance Tube Sample Preparation and Mounting Issues,” *Internoise 2012*, New York City, August 19-22.

Z. Tao, D. W. Herrin and A. F. Seybert, (2003). “Measuring Bulk Properties of Sound-Absorbing Materials Using the Two-Source Method,” *SAE Noise and Vibration Conference and Exhibition*, Traverse City, Michigan, USA, DOI. 2003-01-1586.

H. Utsuno, T. Tanaka, T. Fujikawa, and A. F. Seybert, (1989). “Transfer Function Method for Measuring Characteristic Impedance and Propagation Constant of Porous Materials,” Journal of the Acoustical Society of America **86**(2), 637-643.

H. P. Wallin, U. Carlsson, M. Åbom, H. Bodén and R. Glav, (2011). *Sound and Vibration*, Marcus Wallenberg Laboratory, Stockholm.

C. N. Wang, Y. M. Kuo, and S. K. Chen, (2008). “Effects of Compression on the Sound Absorption of Porous Materials with an Elastic Frame,” Applied Acoustics **69**(1): 31-39.

Q. Wu, (1988). “Empirical Relations Between Acoustical Properties and Flow Resistivity of Porous Plastic Open-Cell Foam,” Applied Acoustics **25**, 141-148.

R. Wu and D. W. Herrin, (2016). “Development of a Rudimentary Materials Database Including Application to the Prediction of Sound Absorptive Performance of Layered Absorbers,” *NoiseCon 2016*, Providence, RI, June 13-15.

R. Wu and D. W. Herrin, (2017). “Utilization of Empirical Models to Determine the Sound Absorption and Bulk Properties of Compressed Materials,” SAE Technical Paper 2017-01-1884, doi: 10.4271/2017-01-1884.

T.G. Zieliński, (2015). “Normalized Inverse Characterization of Sound Absorbing Rigid Porous Media,” Journal of the Acoustical Society of America **137**(6), 3232-3243.

C. Zwikker and C. W. Kosten, *Sound Absorbing Materials* (Elsevier,1949).

.

VITA

Ruimeng Wu was born in Singapore in 1992. He received the Bachelor's degree of science in Mechanical Engineering from Huazhong University of Science and Technology, China in 2013. In August 2013, he enrolled in Department of Mechanical Engineering at University of Kentucky, for graduate study and research assistant. He had a summer internship at Commercial Vehicle Group in 2015 and a summer internship at Blachford Acoustic Laboratory in 2016. During his graduate years at University of Kentucky, he published a "Noise-Con" conference paper and a "SAE Noise and Vibration" conference paper.

.